

- Barth, T.F.W. (1965) On the constitution of the alkali feldspars. *Tschermak's Mineral. Petrogr. Mitt.* 10, 14-33.
- Ferry, J.M. (1980) A case study of the amount and distribution of heat and fluid during a metamorphism. *Contrib. Mineral. Petrol.* 71, 373-385.
- _____. (1981) Petrology of graphitic sulfide-rich schists from south-central Maine: An example of desulfidation during prograde regional metamorphism. *Am. Mineral.* 66, 908-930.
- _____. (1982) Mineral reactions and element migration during metamorphism of calcareous sediments from the Vassalboro Formation, south-central Maine. *Am. Mineral.* 67, in press.
- Ghent, E.D. (1976) Plagioclase-garnet- Al_2SiO_5 -quartz: A potential geobarometer-geothermometer. *Am. Mineral.* 61, 710-714.
- Green, D.H. and A.E. Ringwood (1967) An experimental investigation of the gabbro to eclogite transformation and its petrological applications. *Geochim. Cosmochim. Acta* 31, 767-833.
- Hildebrand, F.B. (1952) *Methods of Applied Mathematics*. Prentice-Hall, Inc., N.Y.
- Laird, J. (1980) Phase equilibria in mafic schist from Vermont. *J. Petrol.* 21, 1-37.
- Liou, J.G., S. Kuniyoshi, and K. Ito (1974) Experimental studies of the phase relations between greenschist and amphibolite in a basaltic system. *Amer. J. Sci.* 274, 613-632.
- Longhi, J. (1976) *Iron, Magnesium, and Silica in Plagioclase*. Ph.D. Thesis, Harvard University, Cambridge, Massachusetts.
- _____, D. Walker, and J.F. Hays (1976) Fe and Mg in plagioclase. *Proc. 7th Lunar Sci. Conf.*, 1281-1300.
- Prigogine, I. and R. Defay (1954) *Chemical Thermodynamics*. (English translation by D.H. Everett) Longmans Green and Co., London.
- Rumble, D., III., J.M. Ferry, T.C. Hoering, and A.J. Boucot (1982) Fluid flow during metamorphism at the Beaver Brook fossil locality, New Hampshire. *Am. J. Sci.* 282, 886-919.
- Thompson, J.B., Jr. (1969) Chemical reactions in crystals. *Am. Mineral.* 54, 341-375.
- _____. (1981) An introduction to the mineralogy and petrology of the biopyriboles. In D.R. Veblen, Ed., *Amphiboles and Other Hydrated Pyriboles - Mineralogy*, Reviews in Mineralogy 9A, 141-188.
- _____, J. Laird, and A.B. Thompson (1982) Reactions in amphibolite, greenschist and blueschist. *J. Petrol.* 23, 1-27.
- Venit, S. and W. Bishop (1981) *Elementary Linear Algebra*. Prindle, Weber and Schmidt, Boston.

LINEAR ALGEBRAIC MANIPULATION of N-DIMENSIONAL COMPOSITION SPACE

F.S. Spear, D. Rumble III, and J.M. Ferry

INTRODUCTION

The purpose of this chapter is to provide a review of the application of linear algebra to petrologic problems. Among the problems faced by petrologists is the graphical representation of the chemical compositions of rocks and minerals. It is a familiar experience that once the number of chemical components in a system exceeds three (or four, at best) visualization of chemographic relations becomes difficult or impossible. Linear algebra, however, provides us with a formalism for dealing with, and extracting information from, n-component chemical analyses. The algebraic approach is completely general and its power extends to systems consisting of any number of components. Moreover, the techniques are not difficult to master, because they are merely an extension of the algebra of a line ($y = mx + b$) to planes and surfaces of n-dimensions.

The main thrust of this chapter will be to attempt to show the relation between the graphical representation of rock and mineral compositions, with which most petrologists are quite familiar, and the formalism of linear algebra. As will be seen, the mathematics are quite simple and, although a knowledge of linear algebra is helpful, it is not essential. Useful textbooks in linear algebra include Aitken (1965), Anton (1973) and Strang (1980); books and articles in the petrologic literature include Korzhinskii (1959), Perry (1967a,b; 1968a,b), Davis (1973) and Greenwood (1967, 1975).

REPRESENTATION OF MINERAL (OR ROCK) COMPOSITIONS IN COMPOSITION SPACE

Composition space is defined as the space whose coordinate axes are the chemical constituents of minerals or rocks (this chapter will deal principally with minerals, but the approach is also applicable to rock compositions). Composition space is completely analogous to physical space where the axes represent units of distance (for example, the number of kilometers in a direction east, north and up), but in composition space the axes represent units of chemical composition (for example, the number of moles of SiO_2 , MgO , and CaO). The units of quantity used for the axes of composition space are completely arbitrary and the choice should depend on the intended use. Molar quantities of oxides are commonly used for minerals and rocks and in this

chapter they will be used exclusively. Other quantities such as grams, weight percent, atoms, and oxygen equivalents are also useful. Brady and Stout (1980) provide an informative discussion on the choice of components in petrologic applications.

There are two common types of coordinate systems to represent composition space in petrology. The most familiar to petrologists is the *barycentric* (center weighted) coordinate system where a two-component system is represented by a line, a three-component system as a triangle and a four-component system as a tetrahedron. Mineral assemblages and rock compositions are most typically represented graphically in barycentric coordinates. The other type of coordinate system is the *Cartesian* coordinate system, which is the conventional orthogonal x-y-z coordinate system. Most algebraic manipulations are done in Cartesian coordinates and the results converted to barycentric coordinates for graphical display.

The first step in applying algebraic methods to composition space is to define the coordinate system and to determine where minerals plot in this coordinate system. The Cartesian coordinate system will be discussed first, and then the relation between the Cartesian and barycentric coordinate systems will be shown.

Figure 1A represents the two-component system, $\text{SiO}_2\text{-MgO}$, in Cartesian coordinates. To determine where a mineral plot simply determine the amount of SiO_2 and MgO in the formula, e.g., quartz plots at (1,0) (i.e., 1.0 SiO_2 and 0.0 MgO), forsterite (Mg_2SiO_4) plots at (1,2), periclase (MgO) plots at (0,1), and enstatite (MgSiO_3) plots at (1,1). Readers familiar with vector notation will recognize that composition is being represented in this coordinate system as a vector, known as *composition vector* of the mineral. Each element of the vector represents the amount of a particular chemical species in the mineral of interest, i.e., ($n[\text{SiO}_2]$, $n[\text{MgO}]$).

Note that the choice of how to write a mineral formula is somewhat arbitrary. For example, enstatite may be written as MgSiO_3 , in which case its vector is (1,1), or as $\text{Mg}_2\text{Si}_2\text{O}_6$, in which case its vector is (2,2). Both of these points are shown in Figure 1A, and it can be seen that En_2 ($\text{Mg}_2\text{Si}_2\text{O}_6$) falls on a line from the origin (0,0) through En_1 (MgSiO_3). Since these are the same material, the conclusion is that in the Cartesian coordinate system it is the direction that the vector points in composition space, not its length, that defines a mineral composition.

The relation between Cartesian and barycentric coordinates is seen in Figure 1B. The latter have the property that the sum of the components

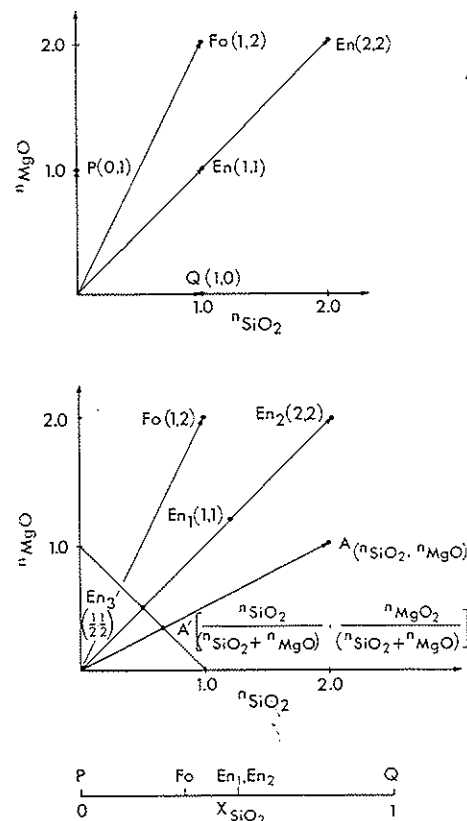


Figure 1. (A) Cartesian coordinate system $\text{SiO}_2\text{-MgO}$ showing plotting positions of periclase (P), forsterite (Fo), enstatite (En_1 ; En_2) and quartz (Q). (B) Diagram showing the relationship between the Cartesian and the barycentric coordinate system, $\text{SiO}_2\text{-MgO}$. The latter is shown as the line between $\text{MgO} = 1.0$ and $\text{SiO}_2 = 1.0$. The plotting positions of the minerals in the barycentric coordinate system are found as the intersection of the mineral vectors with this line (e.g., point En_1 or point A'). (C) Barycentric coordinate system for the system $\text{SiO}_2\text{-MgO}$.

equals 1.0: $\sum X_i = 1.0$. In this two-component system it means that $X(\text{SiO}_2) + X(\text{MgO}) = 1.0$ or $X(\text{MgO}) = 1.0 - X(\text{SiO}_2)$. In the Cartesian coordinate system of Figure 1B, this corresponds to the equation of a line with a slope of -1 between the points (0,1) and (1,0). Thus the barycentric coordinate system is simply the diagonal line between 1.0 MgO and 1.0 SiO_2 .

The plotting position of any mineral in the barycentric coordinate system is the intersection of the vector representing the mineral composition in the Cartesian coordinate system with the line $X(\text{SiO}_2) + X(\text{MgO}) = 1.0$. Since MgSiO_3 and $\text{Mg}_2\text{Si}_2\text{O}_6$ have the same ratio of MgO and SiO_2 , both are represented by vectors that point in the same direction, and both plot at the same point in the barycentric coordinate system. Thus, one property of the barycentric coordinate system is that it preserves the *ratios* of the chemical species in a substance.

The plotting position of a mineral in the barycentric coordinate system can be determined mathematically

by solving for the intersection of the line representing the vector that points to the mineral with the line $\sum X_i = 1$. For an arbitrary mineral with a composition $n(\text{SiO}_2), n(\text{MgO})$ there is a vector that defines a line with the equation (of the form $y = mx + b$),

$$X(\text{MgO}) = \frac{n(\text{MgO})}{n(\text{SiO}_2)} \cdot X(\text{SiO}_2) + 0$$

Solving this equation simultaneously with the equation $X(\text{MgO}) = 1 - X(\text{SiO}_2)$ yields

$$X(\text{MgO}) = \frac{n(\text{MgO})}{n(\text{MgO}) + n(\text{SiO}_2)} \quad \text{and} \quad X(\text{SiO}_2) = \frac{n(\text{SiO}_2)}{n(\text{MgO}) + n(\text{SiO}_2)}$$

Thus the barycentric plotting coordinates of any mineral whose composition is known in Cartesian coordinates can be calculated by normalization.

There are two excellent reasons for using barycentric coordinates in petrology. First, intensive thermodynamic properties of minerals depend not on the absolute number of moles of a species in a substance, but on the mole fraction of a species, and barycentric coordinates deal only with mole fractions. Second, it is possible to graphically represent more composition axes on a piece of paper using barycentric coordinates than it is using Cartesian coordinates. For example, in Figure 1 it takes two dimensions to represent the system SiO_2 -MgO with Cartesian coordinates, but only one dimension (i.e., a line) to represent the system with a barycentric coordinate system (Fig. 1C). Some information is lost in the process (specifically, the absolute amounts of MgO and SiO_2 in our mineral formula), but this is a small price to pay.

It is a simple extension of the above equations to include more components. The mineral or rock compositions are simply represented by vectors with the number of elements in the vectors equal to the number of components in the composition space, each element representing an axis in the Cartesian coordinate system. In this way, composition space of any dimension can easily be represented mathematically, even though only three Cartesian or four barycentric coordinates can actually be drawn.

TRANSFORMATION OF COORDINATE AXES

The transformation of coordinate axes is a mathematical technique of considerable importance to petrology for it can be used to calculate rock norms and end-member mineral components, balance chemical reactions, and compute the plotting coordinates of graphical projections. To transform coordinate axes simply means to compute the elements of a composition vector in terms of any one of several different sets of components that might be chosen. For example, an orthopyroxene solid solution may be expressed in terms of any of the following three sets of components: MgO-FeO- SiO_2 ; Mg_2SiO_4 - Fe_2SiO_4 - SiO_2 ; or MgSiO_3 - FeSiO_3 . Axis transformation, also called linear mapping from one set of coordinates to another, is a fundamental problem of linear algebra, and is treated in all textbooks on the subject (Aitken, 1965; Anton, 1973; Strang, 1980). This procedure is often referred to as the transformation of components from an "old" component set to a "new"

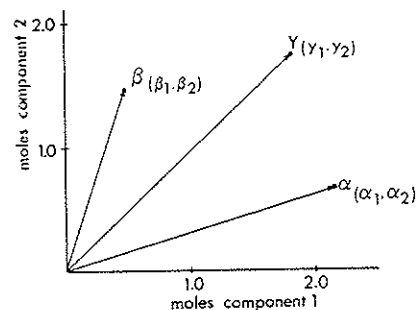


Figure 2. Coordinate system 1 and 2 (the "old" components) showing plotting positions of "new" components α and β and mineral Y , which is to be mapped into the new system α and β .

arals labeled α and β that will serve as "new" coordinate axes (see Fig. 2). The minerals α and β have composition vectors $\alpha = (\alpha_1, \alpha_2)$ and $\beta = (\beta_1, \beta_2)$ in the old coordinate system. Moreover, there is a third mineral Y where $Y = (\gamma_1, \gamma_2)$ that is to be mapped into the "new" coordinate axes α, β . In this and all examples in the chapter it is assumed that the units of quantity for the old and new coordinate systems are the same. But, as pointed out by Brady and Stout (1980, p. 181), this need not be the case, and the units in the old and new systems may be different.

The question asked in this example is: What is the composition vector of mineral Y relative to the coordinate axes α and β ? Or, stated another way: How much of minerals α and β are needed to make mineral Y ? Or, what linear combination of α and β will make mineral Y ? Mathematically, this question is phrased

$$x_1 \cdot \alpha + x_2 \cdot \beta = Y$$

where Y , α , and β are known in the old system, and it is desired to find x_1 and x_2 , which is the solution to where Y plots in the new system. Because this is a two-component system, the above equation actually represents two simultaneous equations:

$$x_1 \cdot \alpha_2 + x_2 \cdot \beta_1 = y_1$$

$$x_1 \cdot \alpha_1 + x_2 \cdot \beta_2 = y_2$$

or, in matrix notation

$$\begin{bmatrix} \alpha_1 & \beta_1 \\ \alpha_2 & \beta_2 \end{bmatrix} \cdot \begin{bmatrix} x_1 \\ x_2 \end{bmatrix} = \begin{bmatrix} y_1 \\ y_2 \end{bmatrix}, \text{ or simply } A \cdot X = Y,$$

component set and has been discussed by Thompson (1957), Greenwood (1975), and Brady and Stout (1980).

The linear mapping of a rock or mineral composition vector from one set of coordinate axes into another set is performed in the following way. First, it is necessary to choose the "new" set of coordinate axes into which the mapping will be done. As an example, let there be a set of axes labeled 1 and 2 (the "old" coordinate system) and two min-

where A is the *coefficients matrix* and X is the *solution vector*.

Since the transformation is made from one set of coordinate axes to another, both of which have the same dimensionality, there will always be the same number of equations as unknowns and the system of equations can easily be solved for X . Note that the *columns* of the coefficient matrix, A , are the composition vectors of the minerals in the new coordinate axes (the "new" components). Also note that each equation has the physical significance of a *mass balance equation* -- that is, equation (1) describes the conservation of component 1 and equation (2) describes the conservation of component 2. Both these equations must be satisfied in the transformation from one component set to another. The solution vector, X , represents the composition vector for mineral Y relative to the new coordinate axes α, β .

To take a more specific example, consider the system SiO_2 - MgO shown in Figure 1. Suppose that we wish to transform this coordinate system into the coordinate system enstatite-periclase, and to map both quartz and forsterite into this new coordinate system. To map quartz, we need to solve the two linear equations

$$x_1 \cdot [\text{En}] + x_2 \cdot [\text{P}] = [\text{Qtz}]$$

or

$$[\text{SiO}_2]x_1 \cdot 1 + x_2 \cdot 0 = 1$$

$$[\text{MgO}] x_1 \cdot 1 + x_2 \cdot 1 = 0$$

where the two equations represent mass balance for SiO_2 and MgO , respectively, as indicated by the square brackets. The two columns of the coefficients matrix are the composition vectors for the new components En and P. Solution of these two equations yields $x_1 = 1$, $x_2 = -1$, which is the composition vector for quartz in the new coordinate system (i.e., $\text{qtz}' = (1, -1)$; the prime notation refers to the composition vector of a mineral in the transformed system). A similar solution to the equation

$$x_1 \cdot [\text{En}] + x_2 \cdot [\text{P}] = [\text{Fo}]$$

or

$$[\text{SiO}_2]x_1 \cdot 1 + x_2 \cdot 0 = 1$$

$$[\text{MgO}] x_1 \cdot 1 + x_2 \cdot 1 = 2$$

yields $\text{Fo}' = (1, 1)$. The minerals En and P could also be mapped from the old system to the new system with the result that $\text{En}' = (1, 0)$ and $\text{P}' = (0, 1)$ as they must, because they are the new coordinate axes.

A plot of the new system is shown in Figure 3A. Note the plotting position of $\text{Qtz}' (1, -1)$. The new barycentric coordinate system can easily

TABLE 1.
Summary of the relationship between the composition vector of a mineral in two-component Cartesian and barycentric coordinate systems.

Sector (Fig. 5)	Sign of elements in Cartesian coordinates	Sum of elements in composition vector	Projects into Barycentric coordinates	Barycentric composition vector
I	(+,+)	+	directly	(+,+)
IIa	(+,-)	+	directly	(+,-)
IIb	(-,+)	+	directly	(-,+)
IIIa	(-,+)	-	through ∞	(+,-)
IIIb	(+,-)	-	through ∞	(-,+)
IIIc	(-,-)	-	through ∞	(+,+)
along line $y=-x$	(\pm, \mp)	0	at ∞	(∞, ∞)

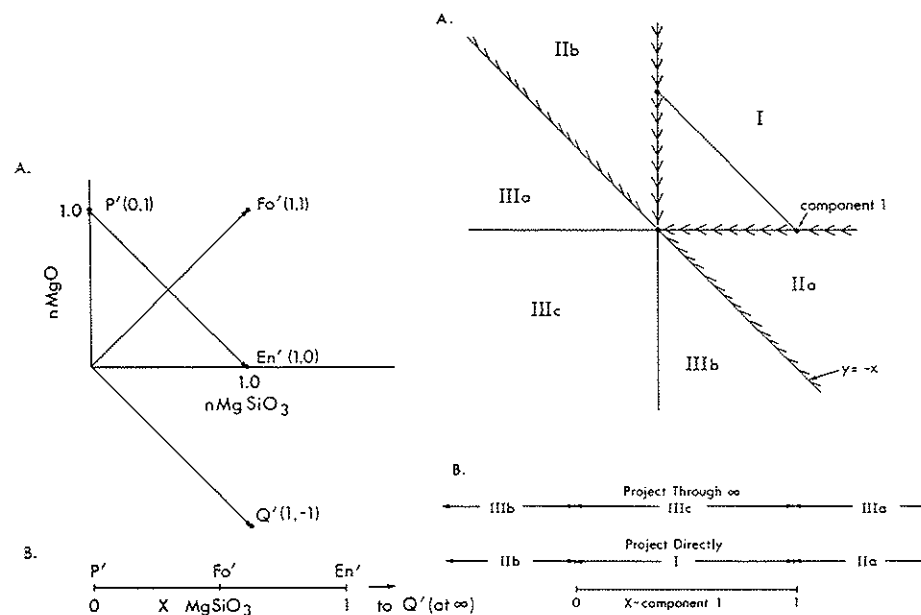


Figure 3, to the left. (A) Plot of the "new" Cartesian coordinate system En-P showing the plotting positions of quartz (Q') and forsterite (Fo') in the new system. Note the plotting position of $Q' (1, -1)$. (B) Barycentric coordinates for the new component system En-P. Note that Q' plots at infinity.

Figure 4, to the right. Cartesian (A) and barycentric (B) coordinate system showing relationship between plotting positions of minerals in the two systems (see text and Table 1).

be calculated by normalizing and is shown in Figure 3B. Thus, in barycentric coordinates, P' plots at (0,1), Fo' plots at $(\frac{1}{2}, \frac{1}{2})$, En' plots at (1,0), but Q' plots at (∞, ∞) . The reason for this can be seen in Figure 3A: The composition vector for Q' (1,-1) is parallel to, and therefore does not intersect, the line for the barycentric coordinate system. Mathematically, this condition of parallelism between the composition vector of a mineral and the barycentric coordinate system arises when the sum of the elements in the composition vector = 0.

In fact, the Cartesian coordinate system can be divided into sectors showing how and where minerals will project into the barycentric coordinate system as shown in Figure 4. All minerals that plot in sectors I, IIa or IIb project directly into the barycentric coordinate system whereas all minerals that plot in sector IIIa, b or c project negatively (through ∞). The line that separates these two regions has the formula $y = -x$. Thus the coordinates of any point that plots along this line has the property that $x + y = 0$, which means that any mineral plotting along this line will have the sum of the elements in its composition vector = 0 and plots at ∞ in the barycentric coordinate system. In sectors I, IIa and IIb, the sum of the elements in the composition vector will be >0 and in sectors IIIa,b,c the sum of the elements will be <0 .

The relationship between the plotting position of minerals in the Cartesian and barycentric coordinates is summarized in Table 1 and Figure 4. As can be seen from the table, there is a direct relationship between the composition vector of minerals in the Cartesian and barycentric coordinates. The *signs* of the elements in the composition vectors are the *same* for minerals that project directly into the barycentric coordinate system (i.e., minerals that plot in sectors I, IIa or IIb); the *signs* of the elements in the barycentric composition vector *change* when the mineral projects through infinity (i.e., minerals that plot in sector IIIa,b,c). If the sum of the elements in the Cartesian coordinate system = 0, the mineral plots at ∞ . This result is valid for composition space of any dimension.

SOLUTION TO THE PROBLEM $A \cdot X = Y$

The linear mapping described in the last section is an extremely powerful and versatile technique for manipulating composition space. In a later section, some examples and applications of this technique will be discussed. In this section, however, some techniques for solving the system of linear

equations will be explored. The purpose of this section is not to provide a discussion of numerical methods, but rather, to show the relationship and similarity among various methods that have been discussed in the literature. For details on the mathematics behind the various methods, the reader is referred to textbooks in linear algebra.

Matrix inversion

A general solution to the system of equations $A \cdot X = Y$ can be obtained by inversion of the coefficients matrix A and post-multiplication by the vector Y. Thus

$$A^{-1}Y = X .$$

Gauss-reduction

This method is a systematic procedure for reducing the system of equations to a form where all of the elements in the coefficients matrix below the diagonal are zero. This is achieved sequentially by adding and subtracting multiples of one equation from another. When all of the elements below the diagonal are zero, the solution can easily be calculated by back substitution.

Cramer's rule

This method utilizes the property that the i^{th} element of the solution vector X (i.e., x_i) is equal to the determinant of the coefficient matrix with the Y vector substituted in for the i^{th} column, divided by the determinant of the entire coefficient matrix. Thus:

$$x_i = \frac{\begin{vmatrix} a_1 & b_1 \dots y_1 \dots r_1 \\ a_2 & b_2 \dots y_2 \dots r_2 \\ a_3 & b_3 \dots y_3 \dots r_3 \\ \cdot & \cdot & \cdot & \cdot \\ \cdot & \cdot & \cdot & \cdot \\ a_r & b_r \dots y_r \dots r_r \end{vmatrix}}{\begin{vmatrix} a_1 & b_1 \dots i_1 \dots r_1 \\ a_2 & b_2 \dots i_2 \dots r_2 \\ a_3 & b_3 \dots i_3 \dots r_3 \\ \cdot & \cdot & \cdot & \cdot \\ \cdot & \cdot & \cdot & \cdot \\ a_r & b_r \dots i_r \dots r_r \end{vmatrix}}$$

Each successive coefficient of the solution vector, x_i , can be obtained by successively substituting the vector Y for different columns in the

coefficient matrix and computing the determinant. Thus the entire solution to the equation $x_1 \cdot \alpha + x_2 \cdot \beta + x_3 \cdot \gamma = Y$ becomes

$$\begin{vmatrix} y_1 & \beta_1 & \gamma_1 \\ y_2 & \beta_2 & \gamma_2 \\ y_3 & \beta_3 & \gamma_3 \end{vmatrix} \cdot \alpha + \begin{vmatrix} \alpha_1 & y_1 & \gamma_1 \\ \alpha_2 & y_2 & \gamma_2 \\ \alpha_3 & y_3 & \gamma_3 \end{vmatrix} \cdot \beta + \begin{vmatrix} \alpha_1 & \beta_1 & y_1 \\ \alpha_2 & \beta_2 & y_2 \\ \alpha_3 & \beta_3 & y_3 \end{vmatrix} \cdot \gamma = Y .$$

$$\begin{vmatrix} \alpha_1 & \beta_1 & \gamma_1 \\ \alpha_2 & \beta_2 & \gamma_2 \\ \alpha_3 & \beta_3 & \gamma_3 \end{vmatrix} \begin{vmatrix} \alpha_1 & y_1 & \gamma_1 \\ \alpha_2 & y_2 & \gamma_2 \\ \alpha_3 & y_3 & \gamma_3 \end{vmatrix} \begin{vmatrix} \alpha_1 & \beta_1 & y_1 \\ \alpha_2 & \beta_2 & y_2 \\ \alpha_3 & \beta_3 & y_3 \end{vmatrix} \cdot Y .$$

Korzhinskii's method

This method was designed specifically for balancing chemical reactions (Korzhinskii, 1959) and is very similar to Cramer's rule except that the entire equation is multiplied by the determinant of the coefficient matrix. The above solution, therefore, becomes

$$\begin{vmatrix} y_1 & \beta_1 & \gamma_1 \\ y_2 & \beta_2 & \gamma_2 \\ y_3 & \beta_3 & \gamma_3 \end{vmatrix} \cdot \alpha + \begin{vmatrix} \alpha_1 & y_1 & \gamma_1 \\ \alpha_2 & y_2 & \gamma_2 \\ \alpha_3 & y_3 & \gamma_3 \end{vmatrix} \cdot \beta + \begin{vmatrix} \alpha_1 & \beta_1 & y_1 \\ \alpha_2 & \beta_2 & y_2 \\ \alpha_3 & \beta_3 & y_3 \end{vmatrix} \cdot \gamma = \begin{vmatrix} \alpha_1 & \beta_1 & \gamma_1 \\ \alpha_2 & \beta_2 & \gamma_2 \\ \alpha_3 & \beta_3 & \gamma_3 \end{vmatrix} \cdot Y .$$

The two solutions are equivalent except for a factor equal to the determinant of the coefficient matrix.

Pros and Cons

The advantages and disadvantages of the different methods principally lie in ease of computation for hand versus computer calculation. Gauss-reduction is particularly straightforward and amenable to hand computation, but Cramer's rule or Korzhinskii's method are both rather simple if the system is small or the coefficient matrix contains a large number of zeros. With a computer the choice is arbitrary, but most computer systems contain "named" matrix inversion routines or routines to solve simultaneous linear equations.

One advantage to Korzhinskii's method, especially for balancing chemical reactions, is in cases where there is a degeneracy in the system. Degenerate systems will be discussed in more detail later, but briefly, if a system is degenerate then the coefficient matrix, A, will be singular, which means that it will not have an inverse and will have a determinant of zero.

Matrix inversion, Cramer's rule, or Gauss-reduction will not yield a solution if there is a degeneracy, but with Korzhinskii's method a solution will

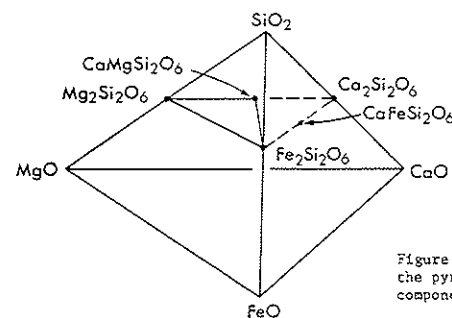


Figure 5. The tetrahedron $\text{SiO}_2\text{-CaO-MgO-FeO}$ showing the pyroxene plane (at $X(\text{SiO}_2) = \frac{1}{2}$) and the "new" components En, Fs, and Di.

still be obtained, except that the coefficient of one of the minerals in the reaction (i.e., one of the "new components") will be zero because the determinant of a singular matrix is zero.

The matrix inversion approach is particularly useful for computer applications where a large number of minerals are to be mapped into a new coordinate system. In this case, the inverse of the coefficient matrix (A^{-1}) can be computed once, yielding a generalized set of equations to map from one coordinate set to another, as has been done by Greenwood (1975).

APPLICATIONS

There are a great number of applications for linear algebra in petrology, some of which will be discussed briefly below. All of the problems involve, in some way, the mapping from one coordinate set into another; the major difference is simply how the original question is formulated.

Calculation of end-member mineral components

This is a straightforward case of mapping a mineral Y, whose composition is known in an old component set (for example, moles of oxides) into a new component set, in this case end-member components. An example involving pyroxenes is shown in Figure 5. The old components in this example are moles of the oxides, $\text{SiO}_2\text{-CaO-MgO-FeO}$, and the new components are the end-members, enstatite ($\text{Mg}_2\text{Si}_2\text{O}_6$), ferrosilite ($\text{Fe}_2\text{Si}_2\text{O}_6$) and diopside ($\text{CaMgSi}_2\text{O}_6$). Note that there are only three linearly independent pyroxene components in the system $\text{SiO}_2\text{-CaO-MgO-FeO}$. (A fourth pyroxene component ($\text{CaFeSi}_2\text{O}_6$) can be calculated as $\text{Di} + \text{Fs} - \text{En}$). However, the choice of which three of the four to pick is completely arbitrary. Note also that there are four "old" components and only 3 "new" components. This is because the pyroxene stoichiometry (sum of the cations = 4) places an additional constraint on

the system. The constraint can be seen in Figure 5: All of the pyroxenes must lie on the plane defined by $X(\text{SiO}_2) = 0.5$. In order to make the transformation, one of two things must be done. An arbitrary "new" component can be added that lies off the pyroxene plane and thus is not a pyroxene end-member (for example, SiO_2). By definition, this component will have a value of 0.0 for any stoichiometric pyroxene. Alternatively, it can be recognized that the only *independently variable* elements in the pyroxene are CaO, MgO and FeO, and the component SiO_2 can be ignored. Adopting the first procedure yields

$$x_1 \text{Qt} + x_2 \text{En} + x_3 \text{Fs} + x_4 \text{Di} = \text{"Px"}$$

$$\begin{aligned} [\text{SiO}_2] \quad & x_1 \cdot 1 + x_2 \cdot 2 + x_3 \cdot 2 + x_4 \cdot 2 = \text{SiO}_2 \text{ in Px} \\ [\text{MgO}] \quad & x_1 \cdot 0 + x_2 \cdot 2 + x_3 \cdot 0 + x_4 \cdot 1 = \text{MgO in Px} \\ [\text{FeO}] \quad & x_1 \cdot 0 + x_2 \cdot 0 + x_3 \cdot 2 + x_4 \cdot 0 = \text{FeO in Px} \\ [\text{CaO}] \quad & x_1 \cdot 0 + x_2 \cdot 0 + x_3 \cdot 0 + x_4 \cdot 1 = \text{CaO in Px} \end{aligned}$$

where x_1 , x_2 , x_3 and x_4 are the amounts of the quartz, enstatite, ferrosilite and diopside components in the pyroxene, respectively. Back substitution quickly reveals that

$$\begin{aligned} x_4 &= \text{CaO in Px} \\ x_3 &= \text{FeO in Px}/2.0 \\ x_2 &= (\text{MgO in Px} - x_4)/2 = (\text{MgO} - \text{CaO})/2.0 \\ x_1 &= \text{SiO}_2 \text{ in Px} - 2x_4 - 2x_3 - 2x_2 \quad \text{or} \\ x_1 &= \text{SiO}_2 - \text{CaO} - \text{FeO} - \text{MgO} \quad \text{or} \\ x_1 &= 0 \text{ (since } \text{SiO}_2 = 2 \text{ and } \text{CaO} + \text{MgO} + \text{FeO} = 2 \text{ in a stoichiometric pyroxene).} \end{aligned}$$

A slightly more complicated example involves the calculation of pyroxene end-member components in the system $\text{SiO}_2\text{-Al}_2\text{O}_3\text{-MgO-FeO-CaO-Na}_2\text{O}$. An arbitrary choice of linearly independent pyroxene end-member components for this system is enstatite ($\text{Mg}_2\text{Si}_2\text{O}_6$), ferrosilite ($\text{Fe}_2\text{Si}_2\text{O}_6$), diopside ($\text{CaMgSi}_2\text{O}_6$), Ca-tschermak's ($\text{CaAlAlSi}_2\text{O}_6$), and jadeite ($\text{NaAlSi}_2\text{O}_6$). Here, the only independently variable cations in the pyroxene are Al(VI), Mg, Fe, Ca and Na, since Al(IV) and Si must be coupled to these cations to maintain electroneutrality and stoichiometry. Hence, there are five equations in five unknowns:

$$x_1 \text{En} + x_2 \text{Fs} + x_3 \text{Di} + x_4 \text{Ct} + x_5 \text{Jd} = \text{Px}$$

$$\begin{aligned} [\text{Mg}] \quad & x_1 \cdot 2 + x_2 \cdot 0 + x_3 \cdot 1 + x_4 \cdot 0 + x_5 \cdot 0 = \text{Mg in Px} \\ [\text{Fe}] \quad & x_1 \cdot 0 + x_2 \cdot 2 + x_3 \cdot 0 + x_4 \cdot 0 + x_5 \cdot 0 = \text{Fe in Px} \\ [\text{Ca}] \quad & x_1 \cdot 0 + x_2 \cdot 0 + x_3 \cdot 1 + x_4 \cdot 1 + x_5 \cdot 0 = \text{Ca in Px} \\ [\text{Al}^{\text{VI}}] \quad & x_1 \cdot 0 + x_2 \cdot 0 + x_3 \cdot 0 + x_4 \cdot 1 + x_5 \cdot 1 = \text{Al(VI) in Px} \\ [\text{Na}] \quad & x_1 \cdot 0 + x_2 \cdot 0 + x_3 \cdot 0 + x_4 \cdot 0 + x_5 \cdot 1 = \text{Na in Px} \end{aligned}$$

or

$$\begin{bmatrix} 2 & 0 & 1 & 0 & 0 \\ 0 & 2 & 0 & 0 & 0 \\ 0 & 0 & 1 & 1 & 0 \\ 0 & 0 & 0 & 1 & 1 \\ 0 & 0 & 0 & 0 & 1 \end{bmatrix} \cdot \begin{bmatrix} x_1 \\ x_2 \\ x_3 \\ x_4 \\ x_5 \end{bmatrix} = \begin{bmatrix} \text{Mg} \\ \text{Fe} \\ \text{Ca} \\ \text{Al(VI)} \\ \text{Na} \end{bmatrix}$$

where x_1 - x_5 are the amounts of the respective components in the pyroxene. Back substitution yields

$$\begin{aligned} x_5 &= \text{Na} \\ x_4 &= \text{Al(VI)} - \text{Na} \\ x_3 &= \text{Ca} + \text{Na} - \text{Al(VI)} \\ x_2 &= \text{Fe}/2 \\ x_1 &= (\text{Mg} - \text{Ca} - \text{Na} + \text{Al(VI)})/2 \end{aligned}$$

An analogous procedure can be followed to calculate end-member components in amphiboles.

Perry (1967a; 1968a,b) has written extensively on the use of algebraic techniques in the classification of minerals and calculating end-member components of minerals. Perry has shown that, in general, 11-dimensional linearly-independent component space is necessary for the description of the chemical variability in feldspars and amphiboles. Moreover, for the amphiboles, there is generally not a set of components whereby all the coefficients of the component set for a particular amphibole have positive values. Negative values of components simply means that the physically accessible composition space of amphiboles cannot be encompassed by a single set of linearly independent end-members. For thermodynamic calculations, however, negative components are perfectly acceptable (cf. Brady, 1975).

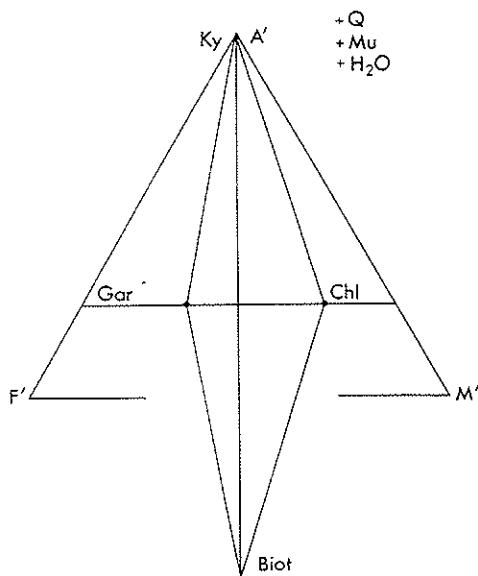


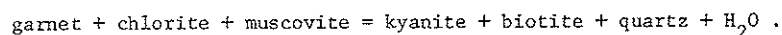
Figure 6. An AFM diagram showing the relationship among the minerals kyanite (Ky), biotite (Biot), chlorite (Chl) and garnet (Gar).

of these minerals is needed to make mineral Y? Or, mathematically, what is the solution (X) to the system of equations:

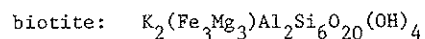
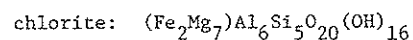
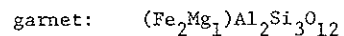
$$x_1 \cdot \alpha + x_2 \cdot \beta + \dots x_n \cdot \gamma = Y?$$

Note that this is exactly the problem of mapping Y into the "new" coordinate system $\alpha, \beta, \dots, \gamma$, and the coefficients of the solution vector X are the stoichiometric coefficients of the reaction. Note also that the above algebraic formulation is consistent with the phase rule, that is, in an n-component system it takes, in general, n+1 phases (e.g., $\alpha, \beta, \dots, \gamma$ and Y) to balance a chemical reaction among the phases (provided there are no degeneracies in the system).

As an example, consider the crossing tie-line relation on the AFM diagram shown in Figure 6, which represents the reaction



The composition of the garnet, chlorite and biotite are



Calculation of rock norms

This problem is exactly analogous to calculating components in minerals except that the total set of normative minerals ("new" components) is not linearly independent. Sequential sets of normative minerals are calculated until all of the coefficients of the composition vector in the new coordinate system are positive.

Balancing chemical reactions

The problem of balancing a chemical reaction among minerals in a system can be formulated as follows: Given the composition of n minerals in an n-component system, what linear combination

Balancing this chemical reaction is equivalent to answering the question: What linear combination of quartz, muscovite, kyanite, chlorite, garnet and H₂O are necessary to make biotite? (Actually, the choice of which mineral to be mapped into the "new" coordinate system is completely arbitrary. Here biotite was chosen, but it could have been any of the six minerals or H₂O.) Mathematically, this is represented by the system of equations:

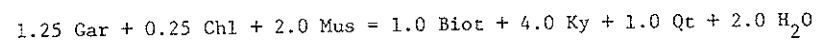
$$x_1 \cdot \text{Qt} + x_2 \cdot \text{Mu} + x_3 \cdot \text{Ky} + x_4 \cdot \text{Ch} + x_5 \cdot \text{Ga} + x_6 \cdot \text{H}_2\text{O} = \text{Biot}$$

[SiO ₂]	$x_1 \cdot 1 + x_2 \cdot 3 + x_3 \cdot 1 + x_4 \cdot 5 + x_5 \cdot 3 + x_6 \cdot 0 = 6.0$
[AlO _{3/2}]	$x_1 \cdot 0 + x_2 \cdot 3 + x_3 \cdot 2 + x_4 \cdot 6 + x_5 \cdot 2 + x_6 \cdot 0 = 2.0$
[FeO]	$x_1 \cdot 0 + x_2 \cdot 0 + x_3 \cdot 0 + x_4 \cdot 2 + x_5 \cdot 2 + x_6 \cdot 0 = 3.0$
[MgO]	$x_1 \cdot 0 + x_2 \cdot 0 + x_3 \cdot 0 + x_4 \cdot 7 + x_5 \cdot 1 + x_6 \cdot 0 = 3.0$
[K ₂ O]	$x_1 \cdot 0 + x_2 \cdot 1 + x_3 \cdot 0 + x_4 \cdot 0 + x_5 \cdot 0 + x_6 \cdot 0 = 2.0$
[H ₂ O]	$x_1 \cdot 0 + x_2 \cdot 1 + x_3 \cdot 0 + x_4 \cdot 8 + x_5 \cdot 0 + x_6 \cdot 1 = 2.0$

or, in matrix notation

$$\begin{bmatrix} 1 & 3 & 1 & 5 & 3 & 0 \\ 0 & 3 & 2 & 6 & 2 & 0 \\ 0 & 0 & 0 & 2 & 2 & 0 \\ 0 & 0 & 0 & 7 & 1 & 0 \\ 0 & 1 & 0 & 0 & 0 & 0 \\ 0 & 1 & 0 & 8 & 0 & 1 \end{bmatrix} \cdot \begin{bmatrix} x_1 \\ x_2 \\ x_3 \\ x_4 \\ x_5 \\ x_6 \end{bmatrix} = \begin{bmatrix} 6.0 \\ 2.0 \\ 3.0 \\ 3.0 \\ 2.0 \\ 2.0 \end{bmatrix}$$

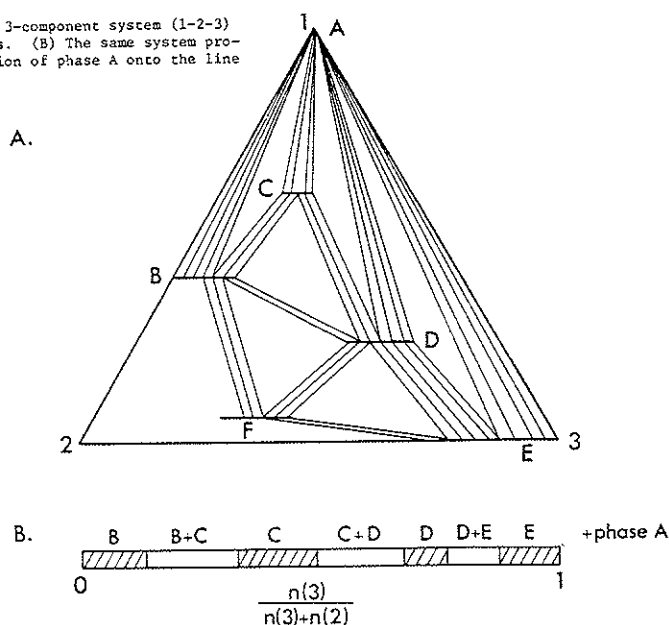
Solution of these equations yields the reaction



where the minerals with negative coefficients have been moved over to the side of the reaction with biotite.

Linear algebra has one of its widest applications in metamorphic petrology in balancing chemical reactions. Korzhinskii (1959) pointed out the utility of linear algebra in balancing petrologic reactions, and the approach has been expanded on by Ferry (1967b). Applications can be divided into two types. The first is where the number of equations is equal to the number of unknowns (that is, the number of phases in the reaction = the number of components + 1) and the solution is exact. This type of problem has greatest application in idealized systems involving end-member components (e.g.,

Figure 7. (A) Schematic 3-component system (1-2-3) showing coexisting phases. (B) The same system projected from the composition of phase A onto the line 2-3.



Perry, 1967a,b; 1968a,b). The second application is where the number of equations exceeds the number of unknowns (the number of phases is less than the number of components + 1) in which case there is no exact solution. In these cases least squares techniques have been employed, as will be discussed in a later section.

Petrologic mixing problems

Mixing problems are exactly analogous to balancing chemical reactions except that these problems usually deal with rock compositions rather than mineral compositions. The problem is usually phrased: How much of the minerals α , β , γ , etc. are necessary to make a rock of composition Y? Clearly, petrologic mixing problems can be formulated in many different ways.

Projective analysis of composition space

Projective analysis is a very powerful technique for the visualization of composition space when the number of components is too large to represent graphically. The goal of projective analysis is to reduce the dimensionality of the composition space by viewing only portions of it at a time--but to do so in such a way that the projected composition space preserves the properties of the full composition space and is thus a rigorous phase diagram in a

thermodynamic sense. Greenwood (1975) has presented an excellent discussion of the mathematics of projective analysis, and the reader is referred to that paper for further discussion (see also Brady and Stout, 1980).

The basis for projective analysis can be seen in diagrammatic form in Figure 7. This figure shows a phase diagram for the three-component system (1-2-3) at some arbitrary but fixed value of pressure (P) and temperature (T). Suppose it was desired to examine the phase relations of only those assemblages in Figure 7 that contained the phase A. Imagine placing one's eye at point A in Figure 7 and sighting down the tie-lines connecting phase A with B, C, and D and E. By continuing these tie-lines down to the join 2-3, the two-component projected phase diagram shown in Figure 7B is obtained. Figure 7B is thus a valid phase diagram for the three-component system 1-2-3 at T and P for all those assemblages that contain phase A.

Mathematically, the plotting positions of minerals B, C and D in the projected composition space 2-3 are easy to calculate by recognizing that the projected plotting coordinates preserve the ratio of components 2 and 3 in the phases (that is, they are projected radially from point A along lines of constant ratio of components 2 and 3). The plotting positions are calculated by simply deleting the element or elements in the transformed composition vector that correspond to the projection point or points (in this case A). The remaining components are then renormalized.

In order to make a projection, it is necessary to have both a projection point and a projection plane (in much the same way that an artist needs a perspective point and a perspective plane to render an accurate perspective drawing). In the above example, the projection point is one of the components of the system (i.e., phase A = component 1) and the projection "plane" is defined by two other components of the system (i.e., the line 2-3). Often, however, the projection point and/or the projection plane are not components of the system to start with, but are the compositions of mineral phases. In order mathematically to make the projection (which simply involves "dropping" the component(s) which represent the projection point(s) and renormalizing), it is first necessary to transform the coordinate system such that the projection point(s) and projection plane are all components of the new coordinate system. This is accomplished quite simply by linear mapping described earlier.

The complete procedure for projective analysis of composition space is:

- (1) Transform the coordinate system so that the axes of the new coordinate system are all either projection points or part of

the projection plane and map all minerals of the system into this new coordinate system.

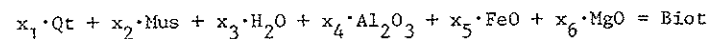
- (2) Perform the projection by "dropping" the components representing the projection points from the transformed composition vectors and renormalize.

It can be seen from Figure 7 that there is a graphical basis for projective analysis. Furthermore, any projected phase diagram will be a valid representation of the phase relations as long as either the projection points are fixed compositions (i.e., not solid solutions) or that all of the projected minerals (e.g., B, C, D, and E) coexist with a phase of the same composition as the projection point. There is also a thermodynamic basis for the validity of the projected composition space. One of the conditions of heterogeneous equilibrium is that the chemical potentials of all components in all phases in an equilibrium assemblage are equal. If one envisions a chemical potential axis coming out of the page in Figure 7A, it will be noticed that all of the minerals that coexist with mineral A (i.e., B, C, D, and E) have the same value for the chemical potential of component 1. In other words,

$$\mu_1^A = \mu_1^B = \mu_1^C = \mu_1^D = \mu_1^E .$$

Hence, the projected phase diagram, Figure 7B, can be seen as a diagram drawn at constant chemical potential of component 1. Chemical potential is an intensive parameter of the system (as are T and P); therefore, a projected phase diagram is valid because it represents mineral coexistences at a constant value of intensive parameters (e.g., T, P and μ_1). This is a requirement of all thermodynamically "legal" projections (Greenwood, 1975).

As an example of the procedure, consider the AFM projection of Thompson (1957). The "old" components are those of the model chemical system for pelitic schists, $\text{SiO}_2\text{-Al}_2\text{O}_3\text{-FeO-MgO-K}_2\text{O-H}_2\text{O}$, and the "new" components include the projection points SiO_2 (quartz), $\text{KAl}_3\text{Si}_3\text{O}_{10}(\text{OH})_2$ (muscovite), and H_2O as well as the projection plane $\text{Al}_2\text{O}_3\text{-FeO-MgO}$. Suppose a plotting position of a particular biotite with the composition $\text{KFe}_{2.5}\text{Mg}_{0.5}\text{AlSi}_3\text{O}_{10}(\text{OH})_2$ on the projection plane $\text{Al}_2\text{O}_3\text{-FeO-MgO}$ is desired. The system of equations looks like:



$$\begin{array}{l} [\text{SiO}_2] \quad x_1 \cdot 1 + x_2 \cdot 3 + x_3 \cdot 0 + x_4 \cdot 0 + x_5 \cdot 0 + x_6 \cdot 0 = 3.0 \\ [\text{Al}_2\text{O}_3] \quad x_1 \cdot 0 + x_2 \cdot 3/2 + x_3 \cdot 0 + x_4 \cdot 1 + x_5 \cdot 0 + x_6 \cdot 0 = 0.5 \\ [\text{MgO}] \quad x_1 \cdot 0 + x_2 \cdot 0 + x_3 \cdot 0 + x_4 \cdot 0 + x_5 \cdot 0 + x_6 \cdot 1 = 0.5 \\ [\text{FeO}] \quad x_1 \cdot 0 + x_2 \cdot 0 + x_3 \cdot 0 + x_4 \cdot 0 + x_5 \cdot 1 + x_6 \cdot 0 = 2.5 \\ [\text{K}_2\text{O}] \quad x_1 \cdot 0 + x_2 \cdot 1/2 + x_3 \cdot 0 + x_4 \cdot 0 + x_5 \cdot 0 + x_6 \cdot 0 = 0.5 \\ [\text{H}_2\text{O}] \quad x_1 \cdot 0 + x_2 \cdot 1 + x_3 \cdot 1 + x_4 \cdot 0 + x_5 \cdot 0 + x_6 \cdot 0 = 1.0 \end{array}$$

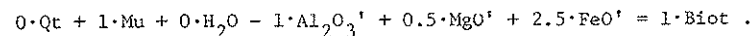
or, in matrix notation ($A \cdot X = Y$)

$$\begin{bmatrix} 1 & 3 & 0 & 0 & 0 & 0 \\ 0 & \frac{3}{2} & 0 & 1 & 0 & 0 \\ 0 & 0 & 0 & 0 & 0 & 1 \\ 0 & 0 & 0 & 0 & 1 & 0 \\ 0 & \frac{1}{2} & 0 & 0 & 0 & 0 \\ 0 & 1 & 1 & 0 & 0 & 0 \end{bmatrix} \cdot \begin{bmatrix} x_1 \\ x_2 \\ x_3 \\ x_4 \\ x_5 \\ x_6 \end{bmatrix} = \begin{bmatrix} 3.0 \\ 0.5 \\ 0.5 \\ 2.5 \\ 0.5 \\ 1.0 \end{bmatrix}$$

The solution ($A^{-1} \cdot Y = X$) is

$$\begin{array}{l} [\text{Qt}] \quad \begin{bmatrix} 1 & 0 & 0 & 0 & -6 & 0 \\ 0 & 0 & 0 & 0 & 2 & 0 \\ 0 & 0 & 0 & 0 & -2 & 1 \\ 0 & 1 & 0 & 0 & -3 & 0 \\ 0 & 0 & 0 & 1 & 0 & 0 \\ 0 & 0 & 1 & 0 & 0 & 0 \end{bmatrix} \begin{bmatrix} 3.0 \\ 0.5 \\ 0.5 \\ 2.5 \\ 0.5 \\ 1.0 \end{bmatrix} = \begin{bmatrix} 0 \\ 1.0 \\ 0 \\ -1.0 \\ 0.5 \\ 2.5 \end{bmatrix} \\ [\text{Mus}] \\ [\text{H}_2\text{O}] \\ [\text{Al}_2\text{O}_3'] \\ [\text{MgO}'] \\ [\text{FeO}'] \end{array}$$

or



Dropping quartz, muscovite, and H_2O as the projection points and renormalizing yields:

$$\text{Biotite} = (-0.5 \cdot \text{Al}_2\text{O}_3', 0.25 \cdot \text{MgO}', 1.25 \cdot \text{FeO}') .$$

One can easily generalize these results to any mineral:

$$\text{Al}_2\text{O}_3' = (\text{Al}_2\text{O}_3 - 3\text{K}_2\text{O}) / (\text{Al}_2\text{O}_3 - 3\text{K}_2\text{O} + \text{FeO} + \text{MgO})$$

$$\text{FeO}' = \text{FeO} / (\text{Al}_2\text{O}_3 - 3\text{K}_2\text{O} + \text{FeO} + \text{MgO})$$

$$\text{MgO}' = \text{MgO} / (\text{Al}_2\text{O}_3 - 3\text{K}_2\text{O} + \text{FeO} + \text{MgO}) .$$

Examples of projective analysis in metamorphic petrology

Since Thompson (1957) presented his AFM projection for muscovite-bearing pelitic schists, graphical analysis of mineral assemblages using thermodynamically legal projections has become an essential tool of the metamorphic petrologist, and application of these techniques has contributed greatly to the understanding of the petrogenesis of metamorphic rocks. Projected phase diagrams are usually three-component triangles, simply because these are easy to draw and visualize. Tetrahedral phase diagrams are also extremely useful because they permit visualization of one more component than a triangle. Tetrahedral phase diagrams can easily be constructed in either perspective or stereoscopic pairs (e.g., Spear, 1980). A computer program for drawing such diagrams is contained in the appendix.

This section will review some of the more commonly used graphical projections and the types of information that have been gained through their application.

Projection involving predominantly pelitic assemblages. Certainly the most widely used graphical projection in metamorphic petrology is Thompson's (1957) AFM projection through the composition of muscovite, quartz, and H₂O. A similar projection for high-grade rocks that contain K-feldspar rather than muscovite was introduced by Barker (1961).

Greenwood (1975) presents three alternative projections of the AFM system that show different portions of composition space. Assuming that it is desirable to retain FeO and MgO as points on the projection plane, three-component phase diagrams can be constructed by projection through one of the following sets of phases:

<u>projection points</u>	<u>projection plane</u>
Quartz, muscovite, H ₂ O	Al ₂ O ₃ '-FeO'-MgO' (AFM)
Al ₂ SiO ₅ , muscovite, H ₂ O	SiO ₂ '-FeO'-MgO'
Al ₂ SiO ₅ , quartz, H ₂ O	Muscovite'-FeO'-MgO'
Quartz, Al ₂ SiO ₅ , muscovite	H ₂ O'-FeO'-MgO'

An example of the last of these projections is shown in Figure 8B (from Greenwood, 1975) along with the conventional AFM diagram (Fig. 8A). The projection in Figure 8B, which is valid for any pelite containing kyanite + quartz + muscovite, depicts the variable H₂O contents of different mineral assemblages at a particular P-T condition. For example, the assemblage

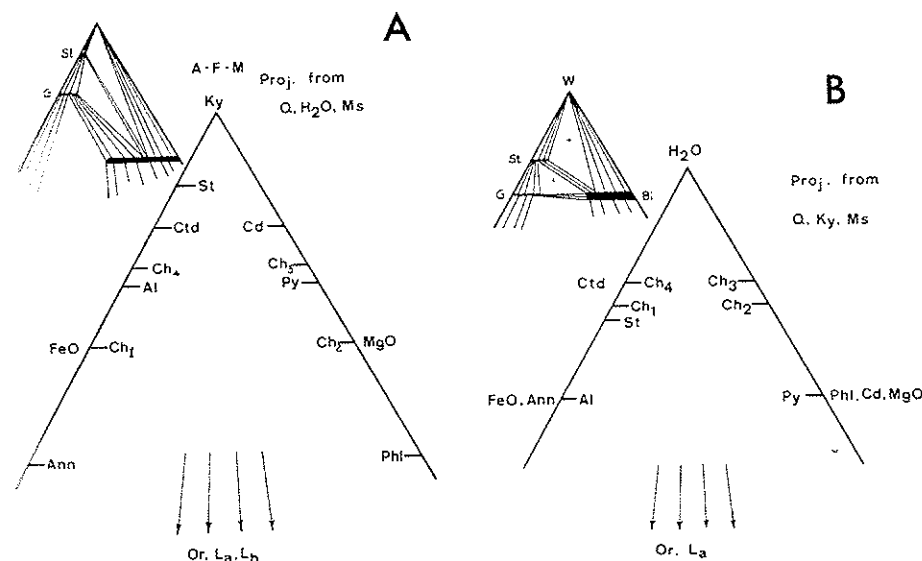


Figure 8. Projections of the six-component pelite system after Greenwood (1975). (A) The AFM projection of J. B. Thompson. The diagram in the upper left corner represents a possible topology at approximately 4 kb and 700°C. (B) Projection of the model pelite system onto the plane H₂O-FeO-MgO from quartz, kyanite and muscovite. Water is shown as an extensive parameter in this diagram in contrast to its role as an intensive variable in Figure 8A. The diagram in the upper left represents a possible topology at approximately 4 kb and 700°C, where Gar-St-Bi are stable with H₂O and Ms, but not with kyanite. In (B) Gar-St-Bi are shown as stable with Q, Ms and Ky but not with pure H₂O. Abbreviations: Ky = kyanite; St = staurolite; Ctd = chloritoid; Cd = cordierite; Ch = chlorite; Al = almandine; Py = pyrope; Ann = annite; Phl = phlogopite; Or = K-feldspar; La and Lb = assumed liquids near the Or-Q-H₂O "eutectic".

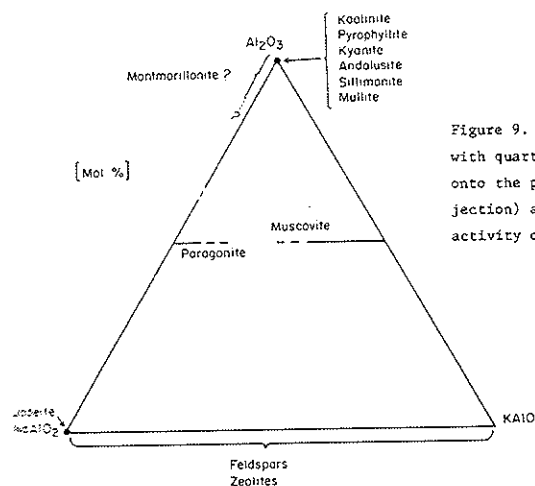


Figure 9. Projection for phases in equilibrium with quartz in the system Na₂O-K₂O-Al₂O₃-SiO₂-H₂O onto the plane NaAlO₂-KAlO₂-Al₂O₃ (the A-K-Na projection) at a given temperature, pressure and activity of H₂O. From Thompson and Thompson (1976).

staurolite + biotite + H₂O (+ quartz + kyanite + muscovite) exists with a pure H₂O fluid, and thus $\mu(\text{H}_2\text{O})$ is defined at a maximum value by this assemblage. Staurolite + biotite (no H₂O) has a lower water content and the assemblage staurolite + biotite + garnet has a still lower H₂O content. Note that this latter assemblage, staurolite + biotite + garnet + quartz + muscovite + kyanite, would appear on a conventional AFM projection as a four-phase assemblage, and is an assemblage which buffers $\mu(\text{H}_2\text{O})$. Projection onto planes containing volatile species, for example, H₂O-FeO-MgO, is an excellent way to visualize the buffering of volatile species by mineral assemblages (see discussion below and Chapter 7 by Rice and Ferry of this volume).

Another useful projection for medium-grade pelitic rocks, which is very similar to the projection discussed above, is a projection through the composition of staurolite, rather than kyanite. This projection has been used quite effectively by Rumble (1977) (see discussion below).

Pelitic schists often contain sodium, and Thompson and Thompson (1976) have discussed facies types in sodium-bearing pelitic schists by consideration of the subsystem SiO₂-Al₂O₃-K₂O-Na₂O-H₂O. Projecting from quartz and H₂O in this system gives the A-K-Na phase diagram shown in Figure 9, which is an adequate representation of this subsystem except in cases where plagioclase contains considerable Ca or muscovite or paragonite contains considerable phengite component. By consideration of naturally-occurring A-K-Na facies types, Thompson and Thompson (1976) derived a petrogenetic grid for this subsystem.

Projections in calcareous bulk compositions. Metamorphosed siliceous dolomitic limestones may be modeled by the system CaO-MgO-SiO₂-H₂O-CO₂. Phase equilibria for this rock type are commonly represented on a CaO-MgO-SiO₂ diagram which is projected through H₂O and CO₂ (Bowen, 1940). Resulting diagrams portray mineral equilibria at constant P, T, $\mu(\text{H}_2\text{O})$, and $\mu(\text{CO}_2)$. Skippen (1974) derived quantitative petrogenetic grids in T-XCO₂ space at several pressures for metamorphosed siliceous dolomitic limestones using the projected CaO-MgO-SiO₂ diagram.

Calc-mica schists and marls can be considerably complex chemically and thus amenable to projective graphical analysis. The premetamorphic protolith of calc-mica schists can be thought of as a calcareous pelite or an alkali-bearing, aluminous carbonate, and it can be represented by the model system SiO₂-Al₂O₃-FeO-MgO-CaO-Na₂O-K₂O-H₂O-CO₂. Thompson (1975), in a study of mineral reactions in a calc-mica schist from Gassetts, Vermont, depicted a

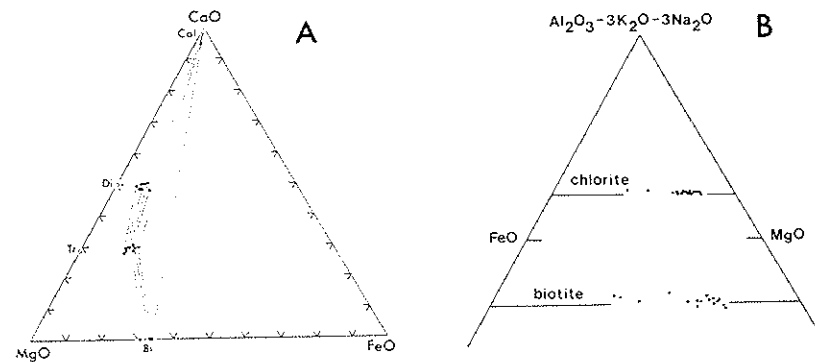


Figure 10. Projections of assemblages in calc-mica schists. (A) From Thompson (1975). Compositions of clinopyroxenes, actinolite, biotite, and calcite (mole percent CaO-MgO-FeO) projected from SiO₂, KAlO₂, H₂O and CO₂. Clinzoisite would plot at CaO if projected from CaAl₂O₆ in addition. (B) From Ferry (1979). Compositions of biotite and chlorite plotted on a diagram that projects through SiO₂, H₂O, KAl₃O₅, and NaAl₃O₅ [biotite and chlorite coexisting with quartz and muscovite of fixed K/Na under conditions of constant P, T, and $\mu(\text{H}_2\text{O})$].

portion of this system by projecting from quartz, KAlO₂, H₂O and CO₂ (Fig. 10A). The diagram in Figure 10A thus refers to mineral assemblages with quartz and K-feldspar at constant P, T, $\mu(\text{H}_2\text{O})$, and $\mu(\text{CO}_2)$. Ferry (1979), in a study of metamorphosed argillaceous carbonate rocks from south-central Maine, utilized a projection through SiO₂, H₂O, KAl₃O₅ and NaAl₃O₅ onto Al₂O₃'-FeO'-MgO' in order to depict composition of coexisting biotite and chlorite (Fig. 10B). The diagram in Figure 10B thus refers to minerals coexisting with quartz and muscovite (with constant K/Na) at conditions of constant P, T, and $\mu(\text{H}_2\text{O})$.

One problem with any graphical representation of phase relations in systems which contain both carbonate and hydrous phases is that most assemblages in these types of rocks buffer $\mu(\text{H}_2\text{O})$ and $\mu(\text{CO}_2)$ rather than vice versa (see Rice and Ferry, this volume). Hence, it is usually impossible to draw a single phase diagram for a wide variety of assemblages.

Projective analysis of amphibolites. These rocks have long defied rigorous projective analysis because of their chemical complexity. The classic ACF diagram of Eskola (1915), while showing the major facies changes, cannot depict the importance of Fe-Mg solution, nor does it adequately account for phase relations involving plagioclase.

Amphibolites can be represented, to a first approximation, by the system SiO₂-Al₂O₃-FeO-MgO-CaO-Na₂O-H₂O. One approach to graphic representation of these rocks has been to project from quartz and H₂O into the tetrahedron Al₂O₃-CaO-Na₂O-(FeO+MgO). This projection obscures the effect of Fe-Mg substitution but is useful for portraying phase relations

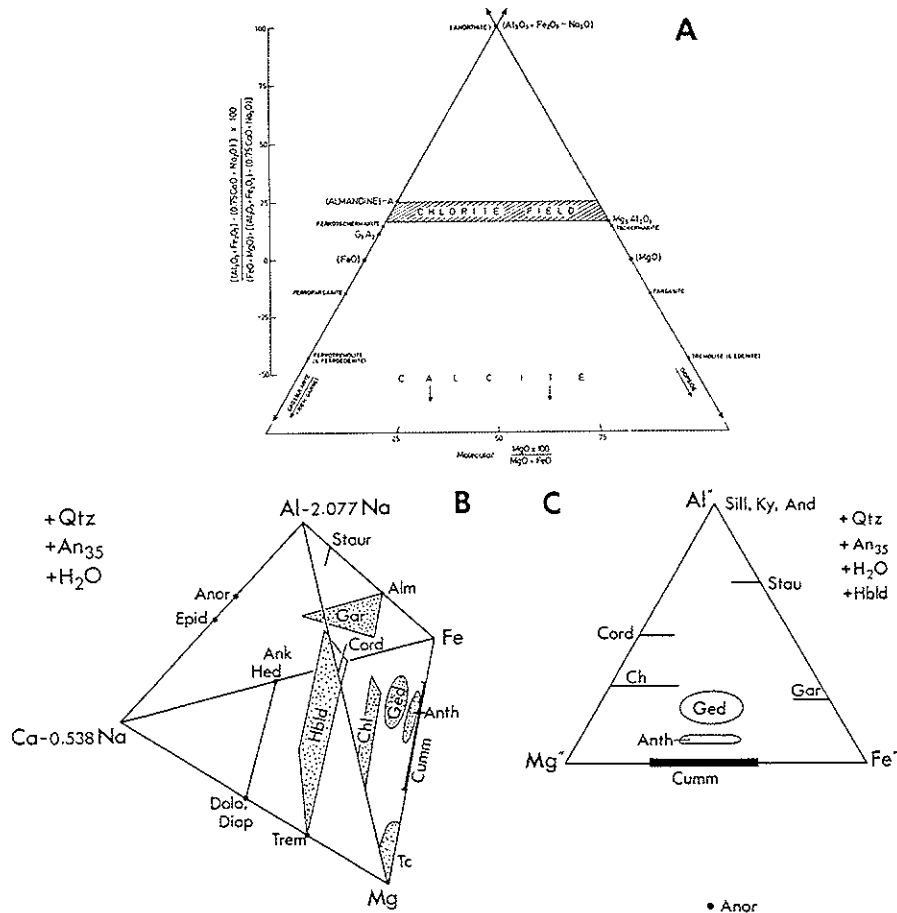


Figure 11. Projections for amphibolite assemblages. (A) From Harte and Graham (1975). Projection from epidote and albite onto the plane $Al_2O_3-FeO-MgO$. This diagram is valid for green-schists and albite-bearing epidote amphibolites. (B) From Spear (1982). Plotting positions for end-member minerals projected from quartz, plagioclase (An_{35}), H_2O , CO_2 into the tetrahedron Fe-Ca-Mg-Al. Abbreviations are: Ged = gedrite; Anth = anchophyllite; Cum = cummingtonite; Chl = chlorite; Tc = talc; Cord = cordierite; Gar = garnet solid solutions; Alm = almandine; Hbl = hornblende; Trem = tremolite; Diop = diopside; Ank = ankerite; Hed = hedenbergite; Epid = epidote (or zoisite); Anor = anorthite; Stau = scapolite. Wonesite, which has not been shown, would plot between talc, chlorite, and cummingtonite but negatively with respect to Ca'. (C) From Spear (1982). Generalized plotting positions of phases projected from quartz, plagioclase (An_{35}), H_2O and 'average' hornblende [$Na_{0.5}Ca_{1.7}Fe_{1.85}Mg_{1.85}Al_{1.4}(Al_{1.5}Si_{1.6}O_{22}(OH)_2$)]. Abbreviations as in (B). This diagram is valid for quartz-, plagioclase-, hornblende-bearing amphibolites.

involving plagioclase. Laird (1980) has made very effective use of this projection in representing phase relations in mafic schist from Vermont. A more rigorous projection was devised by Harte and Graham (1975), who depicted the phase relations of low-grade metabasites from the Dalradian on a type of A'F'M' projection that projects through the compositions of quartz, albite, epidote and H_2O (see Fig. 11A).

Robinson and Jaffe (1969) and Stout (1972) projected orthoamphibole-bearing assemblages from quartz, H_2O , and plagioclase of fixed composition onto the $Al_2O_3-FeO-MgO$ plane. This projection adequately depicts phase relations in low-Ca amphibolites from New Hampshire and southern Norway. Because the projection has the effect of lumping Na and Ca, it does not work well when hornblende coexists with aluminous phases such as staurolite or kyanite, as pointed out by Spear (1982) and Robinson et al. (1981). Spear (1982; see also Robinson et al., 1981) presented an alternative projection from quartz, H_2O , and andesine (An_{35}) into the tetrahedron $Al_2O_3-FeO-MgO-CaO$ (see Fig. 11B). Figure 11B adequately represents phase relations in amphibolites from the Post Pond Volcanics, Vermont, provided only assemblages that crystallized at similar values of $\mu(H_2O)$ are plotted on a single diagram (see below). Spear (1982) has made an additional projection of this system through the composition of hornblende onto the AFM plane (Fig. 11C). Figure 11C can be used as a thermodynamically valid representation of the phase relations in medium-grade, hornblende + andesine + quartz-bearing amphibolites.

Types of information to be gained from graphical analysis. The most obvious benefit of graphical analysis is that it provides a visual representation of mineral phase relations that is considerably easier to comprehend, as well as remember, than mineral analyses or lists of mineral assemblages. But a thermodynamically legal projection is much more than just a diagram. It can represent a phase diagram for complex chemical systems, as discussed in the above examples. It can also provide the basis for a petrogenetic grid for a particular rock type. For example, the grid of Thompson and Thompson (1976) for the A-K-Na facies types or the grids of Albee (1965b), Bass (1969), and Harte (1975) for pelites are all based on projected phase relations.

Perhaps the most extensive use to which projections are put is the testing of validity of the assumptions that go into making the projection. Following Greenwood (1975), the requirement of a thermodynamically legal projection is that "the equilibrium state of the system be uniquely determined by specifying pressure, temperature, and the proportions of the components represented in the diagram. If the diagram is a projection, then the phases or components from which the projection is made must either be present, pure, or have their chemical potentials fixed at a constant value over the whole of the diagram" (Greenwood, 1975, p. 1). If the projected

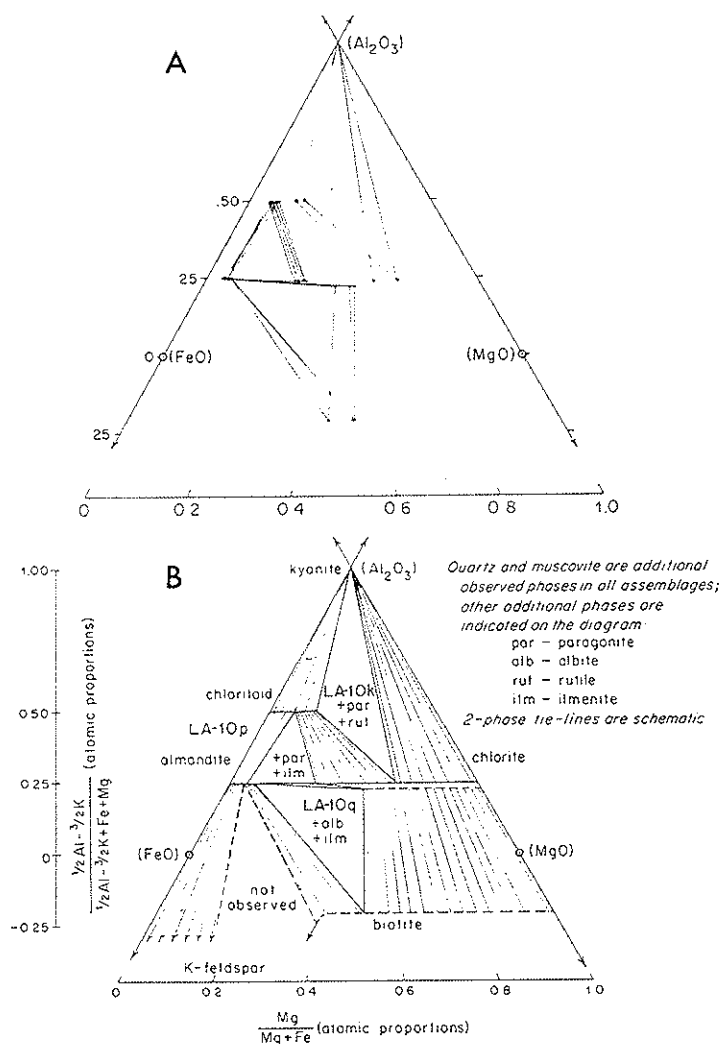


Figure 12. From Albee (1965). Pelitic schist assemblages from Mt. Grant, Vermont. (A) Compositions of coexisting mineral phases shown on a Thompson projection. (B) Observed mineral assemblages and compositions of coexisting phases, shown on a Thompson projection of the $K_2O-Al_2O_3-FeO-MgO$ tetrahedron. Additional accessory phases may include combinations of: hematite, magnetite, apatite, tourmaline, graphite, clinozoisite-allanite, and pyrite.

phase relations of a suite of samples are regular and systematic (with consistent element partitioning and no crossing tie lines or overlapping phase volumes), then it can be concluded that the suite of assemblages are consistent with the above criteria (i.e., that all assemblages equilibrated at the same P, T and chemical potential of projected components). If, however,

crossing tie lines are present, then it can be concluded that a reaction relation existed among the participating assemblages, and one or more of these criteria must be violated.

This type of application has been utilized by many researchers. For example, Albee (1965a), in a classic study of pelitic schists near Mt. Grant, Vermont, used the AFM projection of Thompson (1957) to analyze phase relations in three different assemblages. From the compositions of coexisting minerals (Fig. 12A), Albee deduced the generalized phase relations shown in Figure 12B, and concluded that all assemblages crystallized at the same, P, T, and $\mu(H_2O)$.

On the other hand, Rumble (1977), in a study of metamorphosed pelitic layers from the Clough Formation, New Hampshire, found that phase relations projected onto an AFM diagram (Fig. 13A) were inconsistent with the crystallization of all rocks at the same conditions of P, T, and $\mu(H_2O)$. On the basis of additional projections through the compositions of muscovite, quartz, and either kyanite (Fig. 13B) or staurolite (Fig. 13C) onto the $H_2O-FeO-MgO$ plane, Rumble concluded that assemblages in different beds crystallized at different chemical potentials of H_2O (see also Fig. 13D). A similar conclusion was reached based on phase relations projected through the compositions of quartz, muscovite, staurolite, and magnetite into the $H_2O-FeO-MgO-TiO_2$ tetrahedron. The conclusion was also confirmed by algebraic analysis (see Chapter 4 by Spear et al., this volume).

Spear (1982) presented a graphical analysis of low-variance amphibolite assemblages from the Post Pond Volcanics, Vermont. Figure 14A is a projection of quartz + plagioclase + hornblende-bearing assemblages through the composition of these phases and H_2O on to the plane $AlO_{3/2}-FeO-MgO$. The abundance of four-phase assemblages as well as crossing tie lines suggested that many of these assemblages buffered $\mu(H_2O)$, and that $\mu(H_2O)$ differed from one assemblage to another. Further projection from staurolite (Fig. 14B) as well as algebraic analysis of the phase relations confirmed chemical potential differences in H_2O , as depicted in Figure 14C.

Pitfalls of graphical analysis. Graphical analysis is a very powerful tool, and it is usually the starting point of most phase equilibria studies. It is not, however, without its pitfalls and shortcomings. There are many chemical systems that simply cannot be reduced by projective analysis to a dimension that will permit graphical portrayal. Moreover, it is almost always necessary to ignore or lump "extra" components, which can sometimes lead to erroneous conclusions regarding possible reaction relations. A very

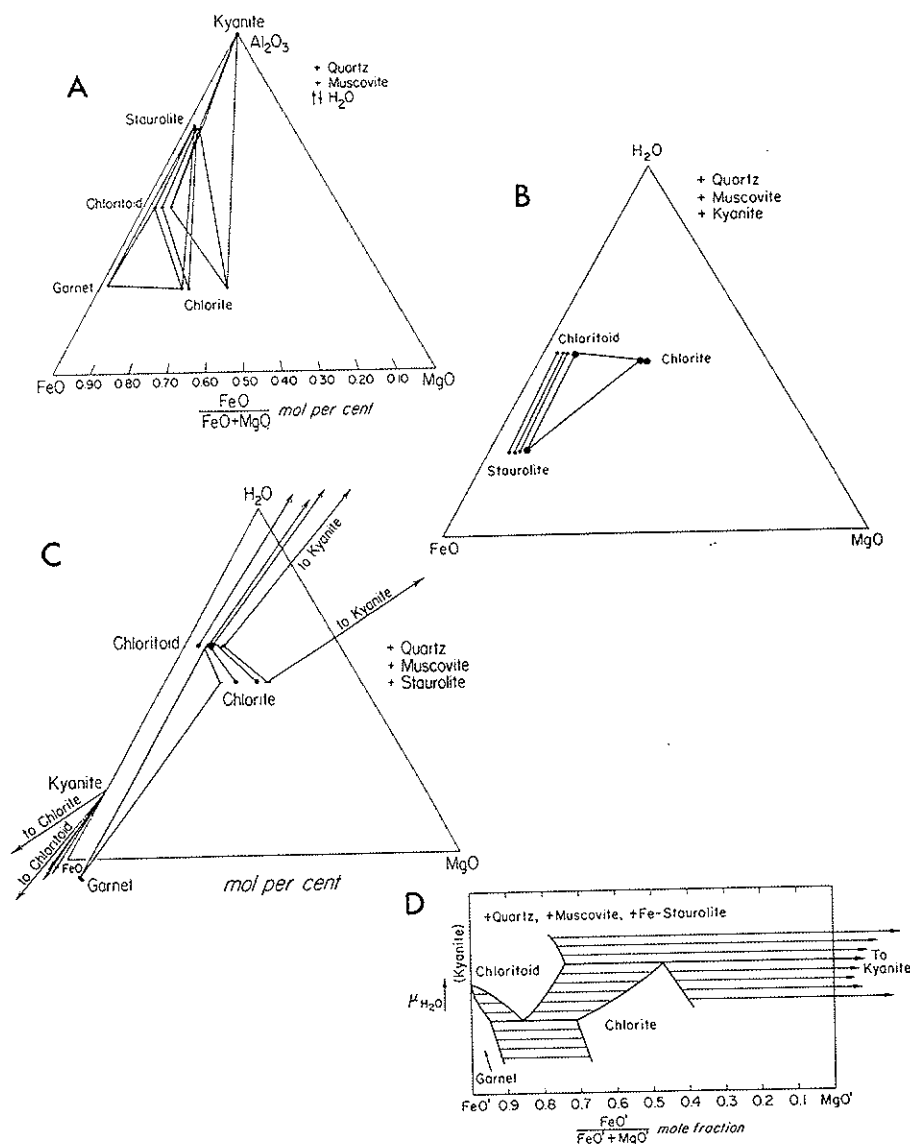


Figure 13. From Rumble (1977). Plotting positions of projected mineral assemblages from Black Mountain, New Hampshire. (A) Kyanite, staurolite, chloritoid, garnet, and chlorite compositions plotted on the AFM projection. The 4-phase assemblage staurolite-chloritoid-garnet-chlorite appears to be an assemblage which buffered $\mu(\text{H}_2\text{O})$. (B) Projection of silicate mineral compositions from quartz, muscovite, and kyanite onto the plane $\text{FeO-MgO-H}_2\text{O}$. (C) Projection of silicate mineral compositions from quartz, muscovite, and staurolite onto the plane $\text{FeO-MgO-H}_2\text{O}$. (D) Isothermal, isobaric, variations of $\mu(\text{H}_2\text{O})$ with mineral assemblage and mineral composition for the system $\text{SiO}_2\text{-Al}_2\text{O}_3\text{-FeO-MgO-K}_2\text{O-H}_2\text{O}$. Constructed from (C) using Korzhinskii's (1959) method of equipotential lines.

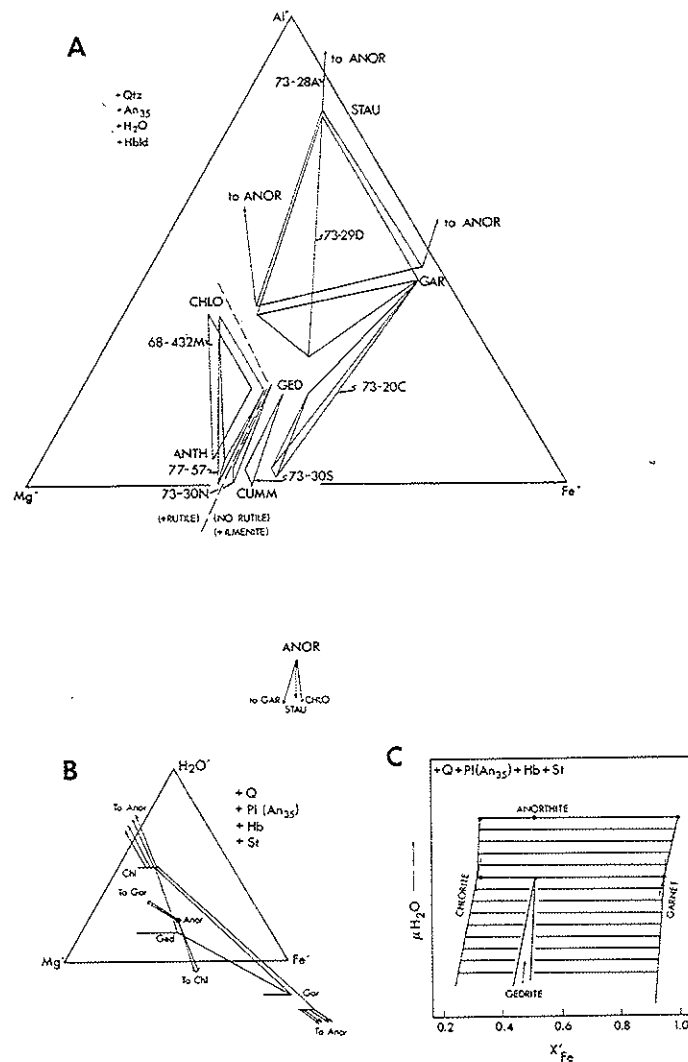


Figure 14. From Spear (1982). Projections of amphibolite assemblages from the Post Pond Volcanics, Vermont. (A) Projection of hornblende-bearing (carbonate-absent) assemblages from quartz, H_2O , An_{35} , and 'average' hornblende onto the plane Al-Fe-Mg . Anorthite projects through infinity; thus tie-lines between anorthite and either chlorite, staurolite, or garnet must project through infinity. Abbreviations as in Figure 11B. The dashed line separates assemblages that contain rutile (the Mg-rich assemblages) from those that contain ilmenite (the Fe-rich assemblages). (B) Projections of the phase relations in (A) through staurolite onto the plane $\text{FeO-MgO-H}_2\text{O}$, depicting the different water contents of the assemblages. (C) $\mu(\text{H}_2\text{O})$ versus X'_{Fe} plot of the assemblages shown in (B).

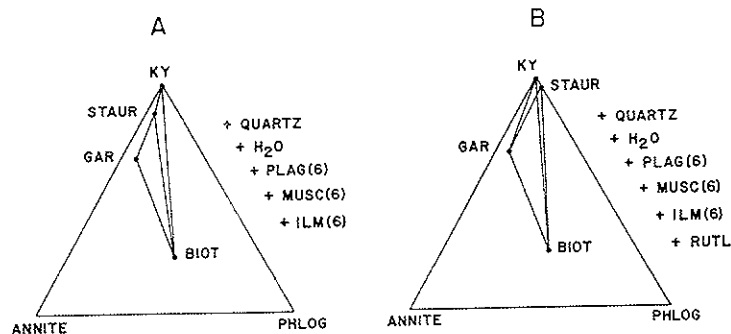


Figure 15. From Fletcher and Greenwood (1979). Projections of phase relations in a specimen of pelitic schist from the Penfold Creek area, British Columbia. (A) Projection from SiO_2 , H_2O , plagioclase, muscovite and ilmenite. Points of projection are those mineral compositions present in the specimen. (B) Projection from SiO_2 , H_2O , plagioclase, muscovite, ilmenite, and rutile. Note that the compositional degeneracy (reaction) inferred from the two projections, which are of the same assemblage, are different. The difference indicates how neglecting to project from a single phase (in this case rutile) can strongly influence resulting conclusions.

revealing example of this type of pitfall is given by Fletcher and Greenwood (1979). Figure 15 shows two projections of phase relations for a sample of pelitic schist; the only difference between the two diagrams is that the diagram on the right is projected from rutile whereas the diagram on the left is not. As can be seen by comparing the two figures, the reaction relation deduced from the two projections is different: Figure 15A suggests staurolite = kyanite + garnet whereas Figure 15B suggests staurolite + garnet = kyanite + biotite. Only the second reaction is correct, as confirmed by linear algebra.

The way around these pitfalls is, of course, not to rely entirely on graphical analysis but to use it as an aid to visualization. The algebraic methods discussed in this chapter and in Chapter 4 by Spear et al. (this volume), permit the same conclusions to be deduced without any simplification resulting from the process of projection.

DEGENERACIES AND LINEAR DEPENDENCIES

It is important to note that the situation sometimes arises in which components chosen for the set of "new" coordinate axes are not all linearly independent. That is, it is possible to make one of these new components out of a linear combination of the other new components. Phrased another way, there is a reaction relationship among the new components. In this case the new coordinate system is said to be degenerate and the coefficients matrix, A, will be singular (i.e., its determinant will be zero and it will not invert). The way to test for a degeneracy is simply to calculate the

determinant of the coefficient matrix A. A zero determinant indicates a singular matrix. A degeneracy may provide important information about the system being studied or it may simply mean that a poor choice of new components has been made.

Linear dependence of component sets

As an example, consider the earlier problem of calculating end-member pyroxene components. It was already stated that in the system SiO_2 - MgO - FeO - CaO , only three pyroxene components are linearly independent (see Fig. 6). However, if we had chosen the four components En, Fs, Di and Hd the transformation matrix would appear as

$$\begin{array}{c}
 [\text{En}] \quad [\text{Fs}] \quad [\text{Di}] \quad [\text{Hd}] \\
 \begin{array}{l}
 [\text{SiO}_2] \\
 [\text{MgO}] \\
 [\text{FeO}] \\
 [\text{CaO}]
 \end{array}
 \begin{bmatrix}
 2 & 2 & 2 & 2 \\
 2 & 0 & 1 & 0 \\
 0 & 2 & 0 & 1 \\
 0 & 0 & 1 & 1
 \end{bmatrix}
 \end{array}$$

The determinant of this matrix is zero, indicating a linear dependence among the new components (i.e., $\text{En} + \text{Hd} = \text{Fs} + \text{Di}$).

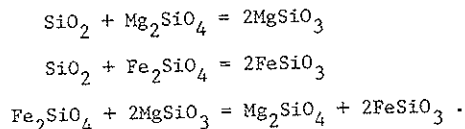
Linear dependence in over- and underdetermined systems

In the above example the number of equations equals the number of unknowns and thus the coefficient matrix is square. However, there are situations where it is desirable to test for linear dependence when the coefficient matrix is not square. For example, many mineral assemblages have a variance greater than two and thus contain more components than phases. Systems such as this where the number of equations exceeds the number of unknowns are called overdetermined. In other situations, the system may contain more unknowns than equations. Systems such as this are called underdetermined. An example of an underdetermined system will be given below.

Testing for linear dependence in overdetermined or underdetermined systems can be done by consideration of a theorem of linear algebra which states that if a matrix is singular, then the matrix obtained by post multiplication of the singular matrix by any other matrix will also be singular. A convenient matrix to multiply the singular matrix by is the transpose of the singular matrix (the transpose of a matrix is simply the matrix with the columns and rows exchanged and is denoted as A^T). Therefore, if A is

singular, then AA^T will also be singular. Because A is an $n \times m$ matrix, the transpose of A is an $m \times n$ matrix and AA^T is an $n \times n$ square matrix. We can easily test for linear dependence in AA^T by calculating the determinant.

As an example, consider the situation described in "Algebraic Formulation of Phase Equilibria" (Spear et al., Chapter 4, this volume) in which we wish to know whether or not a system of equilibrium relations are linearly independent. The three equilibrium relations are



In this example, it is clear that there is a linear dependence, but it is not always so obvious. The problem is formulated algebraically by first writing the three equations with all phases on one side of the equals sign:

$$\begin{aligned} 0 &= \text{SiO}_2 + \text{Mg}_2\text{SiO}_4 - 2\text{MgSiO}_3 \\ 0 &= \text{SiO}_2 + \text{Fe}_2\text{SiO}_4 - 2\text{FeSiO}_3 \\ 0 &= \text{Fe}_2\text{SiO}_4 - \text{Mg}_2\text{SiO}_4 - 2\text{FeSiO}_3 + 2\text{MgSiO}_3 \end{aligned}$$

The coefficient matrix, A, contains the coefficient of each mineral in the three reactions. A is therefore a 3×5 matrix and AA^T is computed as:

$$\begin{array}{c} \text{A} \\ \text{Q} \quad \text{Fa} \quad \text{Fo} \quad \text{Fs} \quad \text{En} \\ \left| \begin{array}{ccccc} 1 & 0 & 1 & 0 & -2 \\ 1 & 1 & 0 & -2 & 0 \\ 0 & 1 & -1 & -2 & 2 \end{array} \right| = \begin{array}{c} \text{A}^T \\ \left| \begin{array}{ccc} 1 & 1 & 0 \\ 0 & 1 & 1 \\ 1 & 0 & -1 \\ 0 & -2 & -2 \\ -2 & 0 & 2 \end{array} \right| = \begin{array}{c} \text{AA}^T \\ \left| \begin{array}{ccc} 6 & 1 & -5 \\ 1 & 6 & 5 \\ -5 & 5 & 10 \end{array} \right| \end{array} \end{array}$$

The determinant of AA^T is zero and thus a linear dependence exists among these three equations. Specifically, the third equation can be obtained by subtracting the second equation from the first.

Linear dependence and the variance of a mineral assemblage

One particularly useful application for the above test for linear independence is in consideration of the variance of a mineral assemblage. The variance, as calculated from the phase rule ($F = C + 2 - P$), is only valid if there are no linear dependencies (i.e., compositional degeneracies) in

the system. Linear algebra provides a way to test for linear dependencies in a particular mineral assemblage and thus examine whether the phase rule variance applies. The necessary criterion for no linear dependencies in a mineral assemblage is either (a) that the determinant of the coefficient matrix not be zero or (b) for assemblages where there are more components than phases, that the determinant of $A^T A$ not be zero.

This procedure tests for exact compositional degeneracies (that is, whether a chemical reaction written among phases of the assemblage balance exactly). It is also possible to test for the existence of compositional degeneracies within the error of an electron microprobe analysis by the method of least squares, as suggested by Greenwood (1968) (see also Pigage, 1976, and discussion below).

TREATMENT OF "EXTRA" COMPONENTS

Quite often it is found that a measured mineral or rock composition contains elements that are not considered as part of the "model" rock system. For example, a model pelitic schist contains the components SiO_2 - Al_2O_3 - FeO - MgO - K_2O - H_2O , but the components CaO , MnO , TiO_2 , ZnO and Na_2O are commonly present in significant quantities in certain phases (e.g., Zn in staurolite; Mn or Ca in garnet; Na in white micas).

When there is a sufficient quantity of an "extra" component to stabilize an extra phase, for example TiO_2 stabilizing ilmenite or rutile or Na_2O stabilizing paragonite or albite, then this phase may be used as one of the "new" coordinate axes and either projected from, if graphical analysis is the goal, or used in balancing a chemical reaction. If, however, no new phase is stabilized, then the problem is how to treat the "extra" components. Mathematically, the problem is equivalent to transforming from an "old" set of coordinate axes with dimensionality n to a "new" set of coordinate axes with dimensionality less than n . That is, we are transforming from a higher order space into a lower order space. Thus, when the transformation matrix is set up, it will be seen that there are a greater number of equations than unknowns and that the transformation matrix is overdetermined. (Singularities in overdetermined systems were discussed briefly in the previous section.)

There are three common ways to handle the overdetermined transformation:

- (1) Ignore the component entirely and recalculate the analysis as if the component were not present. This is effectively the same as projecting through the component.

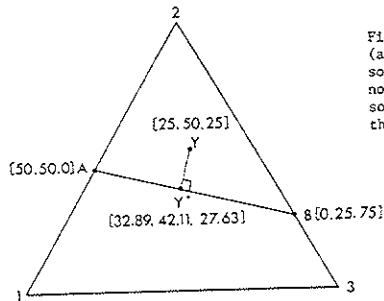


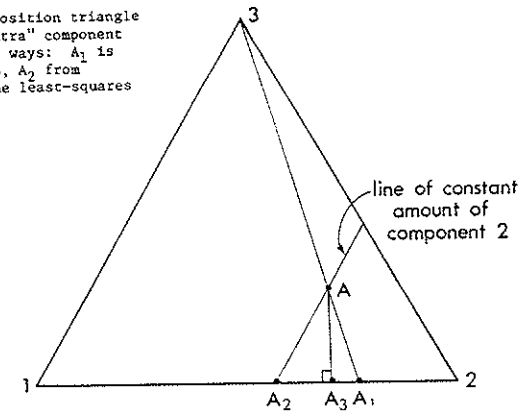
Figure 16. Schematic 3-component composition diagram (after Greenwood, 1968) showing the least-squares solution to the equation $x_1A + x_2B = Y$ where Y does not fall on the line A-B. Y^* is the least-squares solution and represents the point along the line A-B that is closest to Y .

- (2) Lump the extra component together with another component, especially one that behaves in a similar crystal chemical fashion. For example, lump MnO with FeO or lump Fe_2O_3 with Al_2O_3 .
- (3) Model the measured mineral composition by least squares approximation. Least squares provides a solution to the problem of linear mapping from a higher order space into a lower order space. For example, in Figure 16, the mineral Y is contained in the three-component system (1-2-3) and we wish to map Y into the two-component "new" system consisting of A-B (A and B might be end-member mineral formulas or perhaps we wish to balance the chemical reaction $A + B = Y$). As can be seen in Figure 16, mineral Y lies outside of the two-component space defined by A-B; thus, to perform the mapping we must somehow reduce the dimensionality of the space.

The least squares solution is the unique linear combination of the "new" components (A and B in this example) that *most closely approximates* the composition of the mineral that is being mapped. In Figure 16, Y is the mineral being mapped and Y^* is the least squares solution. Y^* falls along the line that joins A and B at a point that is closest to point Y . Thus, Y^* defines the point where the length of the vector between Y and the join A-B is shortest (i.e., the shortest residual vector). The angle $A-Y^*-Y$ must be 90° . Some computational aspects of least-squares modeling are discussed in the next section.

The graphical effect of discarding, lumping and least-squares modeling can be seen in Figure 17. In this example, the "model" system consists of components 1 and 2, and the "extra" component is 3. Discarding component 3 from phase A is equivalent to projecting from component 3 and results in point A plotting at A_1 along the join 1-2. Note that this procedure preserves

Figure 17. Schematic 3-component composition triangle showing the result of removing the "extra" component (3) from mineral A in three different ways: A_1 is the result from discarding component 3, A_2 from lumping with component 1, and A_3 is the least-squares approximation.



the ratio of components 1:2. Lumping component 3 with another component (say, with component 1) does not change the absolute amounts of the other components; hence, point A_2 is found by moving along a line of constant amount of component 2 to the join 1-2. Note that this procedure destroys the original ratio of 1:2. The least-squares approximation is point A_3 and is found by dropping a normal from point A to the 1-2 join.

The three methods quite obviously do not result in the same projected plotting position for point A. Point A_3 is closest in absolute magnitude to point A, point A_1 preserves the original ratio of 1:2, but point A_2 may be desirable for crystal-chemical reasons. Note that as the amount of component 3 in phase A increases, the discrepancy between the points A_1 , A_2 and A_3 increases. Unfortunately, there is no "correct" way to handle extra components; all three methods result in simplifications that will alter the appearance of the phase diagram of the sub-system relative to the model system.

LEAST-SQUARES MODELING IN PETROLOGY

Least-squares solutions to petrologic problems have had considerable application in petrology and deserve some discussion. A detailed discussion of the theory of least-squares modeling is beyond the scope of this paper, however, and the reader is referred to excellent textbooks on the subject for further information (e.g., Davis, 1973; Draper and Smith, 1966).

As outlined in the previous section, the least-squares approach is applicable in overdetermined systems where a mineral or rock is to be mapped from a higher order composition space into a lower order space. The least-squares solution is a "model" composition contained wholly in the lower

order space. This "model" composition is defined as the composition in the lower order space that is closest in distance to the actual mineral composition. That is, the length of the vector connecting the "model" composition and the actual composition is minimized. This vector is called the residual vector, R, and is defined as $R = Y^* - Y$ where Y^* is the model and Y is the actual composition. Formally, the least-squares solution minimizes $\sum R_i^2$ (the sum of the squares of the residuals), which is also equivalent to the length of R (the dot product of R on itself). Hence, both are minimized by the least-squares solution.

As an illustration of the application of least-squares modeling to petrology, consider the example of Greenwood (1968) (see Fig. 16). The two minerals A and B have compositions (50,50,0) and (0,25,75), respectively, and the mineral Y has a composition (25,50,25). The problem is to balance the equation $X_1A + X_2B = Y$, which is equivalent to performing a linear mapping of Y into the new coordinate system A,B. Clearly, this cannot be done exactly because Y does not fall on the line connecting A and B. The least-squares solution to this problem is the model composition Y^* , which can be found graphically by finding the normal to the line A-B that passes through Y.

Mathematically, this problem can be expressed as follows. The mass balance equation to be solved is

$$\begin{aligned} X_1 \cdot A + X_2 \cdot B &= Y + R \\ \hline X_1 \cdot 50 + X_2 \cdot 0 &= 25 + R_1 \\ X_1 \cdot 50 + X_2 \cdot 25 &= 50 + R_2 \\ X_1 \cdot 0 + X_2 \cdot 75 &= 25 + R_3 \end{aligned}$$

where R is the residual vector $Y^* - Y$, or in matrix notation,

$$A \cdot X = Y + R.$$

The vector R is required to make this equation exact. The least-squares solution is given by

$$X = (A^T \cdot A)^{-1} A^T \cdot Y$$

where A^T is the transpose of A. For the above example, $X = (0.658, 0.368)$. The model composition, Y^* , is then calculated simply as

$$A \cdot X = Y^*$$

or $Y^* = (32.89, 42.11, 27.63)$ with a residual vector $R = (7.89, -7.89, 2.63)$

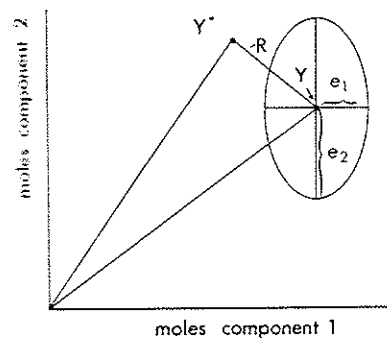


Figure 18. Schematic representation of the least-squares solution (in Cartesian coordinates) showing the model composition, Y^* , the actual mineral composition, Y, the residual vector, R, and the error ellipsoid defined by the error vector, E.

(note that this result is slightly different from that obtained by Greenwood, 1968).

One particular advantage to the least-squares approach is that it permits evaluation of the statistical significance of the solution obtained. This is particularly important when dealing with real mineral compositions. For example, if the mineral Y is analyzed by conventional techniques such as the electron microprobe, the composition of Y will have an error associated with each component, which can be denoted by an error vector, $E_Y = (e_1, e_2, e_3 \dots e_n)$. Each element in the error vector is the standard deviation of the measurement of the i^{th} element of the vector Y. If the minerals A and B are also measured by chemical analysis, as opposed to being fixed, end-member components, then there is also an error vector associated with each of these vectors, E_A and E_B . Hence, there is also an error associated with the model composition, Y^* . These error vectors can be combined into a single error vector that is the sum of the error on Y and the weighted sum of the error on A and B (that is, weighted by the least-squares solution, X). In other words,

$$E = E_Y + X_1 \cdot E_A + X_2 \cdot E_B.$$

This error vector then represents the total error in measurement associated with Y and Y^* , and it can be compared directly with R. This error vector defines an error ellipsoid around Y (or Y^*) where each element of E is the length of one of the axes of the ellipsoid (see Fig. 18) (note that an alternative approach is to draw two error ellipsoids, one around Y ($= E_Y$) and one around Y^* ($= X_1 \cdot E_A + X_2 \cdot E_B$), as has been done by Greenwood, 1968). This error ellipsoid can then be compared directly with R to determine whether or not Y^* falls within the error ellipsoid of Y. This can be determined by computing the length of the vector R, which is the distance between Y^* and Y,

and comparing it with the size of the error ellipsoid in the direction of R. If this distance is greater than the length of R, then Y* is inside the error ellipsoid; otherwise, it is outside. For example, in Figure 18 the model Y* is outside the error ellipsoid.

The procedure of determining whether or not Y* is within the error ellipsoid permits evaluation of the quality of the least-squares model Y* as a statistically significant model of Y. If Y* is within the ellipsoid, then Y* is a significant model of Y within one standard deviation of the measurement on Y, A, and B. Quite obviously, the quality of Y* as a significant model of Y will depend directly on the errors associated with measurement of Y, A, and B.

The above example is an unweighted, unconstrained least-square problem, but it is also possible to weight the mass balance equations in the least-squares solution or to impose any number of constraints on the solution. Reid et al. (1973) have presented a generalized model for constrained least-squares problems. They stress the importance of careful examination of the physical meaning of the mixing model and state that meaningful models can only be obtained by properly weighting the equations, by constraining the solution, and by analyzing the uncertainties in the values of the parameters.

As pointed out by Reid et al., a rigorous solution to the weighted least-squares problem requires knowledge of the variance-covariance matrix. The variance-covariance matrix, C, is a matrix that contains the variance (standard deviations) of the measurements of each component as diagonal elements of the matrix and the covariance of the ith measurement with the jth measurement as the off diagonal elements. For example,

$$C = \begin{vmatrix} \sigma_1^2 & \sigma_{12}^2 & \sigma_{13}^2 & \sigma_{14}^2 & \dots & \sigma_{1n}^2 \\ \sigma_{21}^2 & \sigma_2^2 & \dots & \dots & \dots & \dots \\ \cdot & \cdot & \dots & \dots & \dots & \cdot \\ \cdot & \cdot & \dots & \dots & \dots & \cdot \\ \sigma_{n1}^2 & \sigma_{n2}^2 & \dots & \dots & \dots & \sigma_n^2 \end{vmatrix}$$

The solution to the weighted least-squares problem when the variance-covariance matrix is known is

$$X = (A^T \cdot C^{-1} \cdot A)^{-1} \cdot A^T \cdot C^{-1} \cdot Y .$$

Note that if the variance-covariance matrix equals the identity matrix, the weighted least-squares solution reduces to the unweighted solution.

Knowledge of the covariance of measurements used in petrologic mixing problems is usually not available. If one is dealing with mineral compositions determined from electron microprobe analysis, it is usually assumed that the measurement of one element is unaffected by the amounts of other elements, but this is clearly not true because absorption and fluorescence corrections (e.g., Bence and Albee, 1968) are dependent to a first order on the concentration of all other elements, as is the normalization of formula units. Moreover, in real mineral systems, elemental abundances are constrained by the crystal chemistry of the phase. For example, in plagioclase, as Na and Si increase, Ca and Al must decrease. To our knowledge, however, a rigorous analysis of covariance for mineral analyses has never been presented.

Reid et al. (1975) suggest that, for analytical techniques such as electron microprobe analysis, the covariance is probably small and the variance of the measurements can be used as weighting factors. In this case, the variance-covariance matrix becomes a diagonal matrix (off diagonal elements = 0) with the diagonal elements equal to the square of the standard deviation of the measurements.

Reid et al. stress the importance of proper weighting. If no weighting is used, equal absolute errors are assumed and the solution is dominated by the mass balance equation for the most abundant elements. Weighting has the effect of increasing the importance of minor components in the regression.

One additional aspect of weighted least squares needs to be discussed. As pointed out earlier, in most petrologic mixing problems there are not only errors in the mineral composition to be modelled (Y) but also in the mineral compositions in the coefficients matrix (A). These errors should also be considered in the weighting procedure and an algorithm for doing so was suggested by Reid et al. and Albarede and Provost (1977). The algorithm involves an iterative solution whereby in each iteration the weighting factors are recomputed as the error on Y plus the sum of the errors on the coefficients matrix, weighted by the previous least-squares solution. Pigage (1982) has employed this algorithm in calculations and states that it gives results similar to the standard weighted least-squares technique.

It is often necessary to impose constraints on least-squares solutions in order that the solution have physical meaning, as discussed by Reid et al., Albarede and Provost, and LeMaitre (1979). LeMaitre, for example, has discussed the advisability of imposing the constraint $\sum X_i = 1.0$ on any

least-squares solution involving mineral or rock compositions. For further discussions of constrained least-squares problems, the reader is referred to these papers.

Application of least-squares modeling to petrology

Least-squares modeling in metamorphic petrology has had principal application in solving mass balance equations with specific application to problems such as balancing chemical reactions, determining compositional overlap between mineral assemblages (the n-dimensional tie-line problem), and modal analysis. Other applications include derivation of thermochemical data from reversed experimental studies.

Balancing chemical reactions and the n-dimensional tie-line problem.

Greenwood (1967,1968) discussed the problem of whether or not tie lines cross in n-dimensional space and presented an algorithm to solve this based on least-squares modeling (Greenwood, 1968; Greenwood, 1967, used a linear programming technique to solve the n-dimensional tie-line problem). The essence of Greenwood's argument is that if tie lines between two assemblages cross (or n-dimensional phase volumes intersect) then there will be a reaction relationship between the two assemblages of the form

$$X_1A_1 + X_2A_2 + X_3A_3 = Y_1B_1 + Y_2B_2 + Y_3B_3$$

where the minerals A_1, A_2, A_3 and B_1, B_2, B_3 belong to the two different assemblages. This equation can be expressed as

$$B_1 = Z_1A_1 + Z_2A_2 + Z_3A_3 + Z_4B_2 + Z_5B_3$$

where coefficients Z_1, Z_2 and Z_3 are positive and Z_4 and Z_5 are negative. This equation is a system of mass balance equations of the form $A \cdot X = Y$ and is directly amenable to solution by least-squares techniques. The model composition Y^* can be compared directly with Y to determine if the difference (i.e., R) is within the errors estimated from electron microprobe analysis.

This approach is, of course, not simply restricted to the n-dimensional tie line problem, but is applicable to the modeling of any type of metamorphic reaction. Greenwood (1968) tested his approach through an analysis of the data of Engel and Engel (1962a,b) pertaining to the amphibolite to granulite facies transition in the Northwest Adirondacks of New York State. Greenwood found that it was impossible to relate the mineral assemblages of the Emmeryville Area (amphibolite facies) to those of the Colton Area (granulite facies) by simple mass balance equations. The difference between the mineral assemblages in hornblende amphibolite and in pyroxene granulite

must be due, at least in part, to changes in bulk rock composition, as well as changes in P and T . In other words, the metamorphism cannot be considered to be isochemical, at least for the samples analyzed by Greenwood.

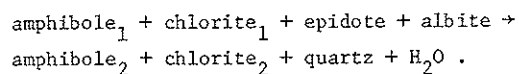
Fletcher (1976) examined possible reaction relations in a finely banded, two-pyroxene amphibolite from southeastern Ontario. All of the samples studied by Fletcher were from a very small outcrop where T and P could be assumed to have been constant. The effects of bulk composition on mineral assemblage therefore could be analyzed separately from the effects of P and T . No reaction relations could be found between many of the samples, and the mineralogical differences were attributed to differences in bulk compositions. Between several of the assemblages, however, it was found that reaction relations did, in fact, exist, which could only be explained by differences in the H_2O -content between assemblages. It was therefore concluded that several of the amphibole-two pyroxene assemblages acted as H_2O -buffers during metamorphism.

Pigage (1976), in a study of pelitic schists from southern British Columbia, was able to document through his regression analysis that the assemblage staurolite + kyanite + garnet + biotite + muscovite + quartz + plagioclase + ilmenite + rutile, which appears as a four-phase assemblage on an AFM projection, acted as an H_2O -buffer. This assemblage could have existed over the P - T interval observed in the field only if $P(H_2O) < P_{total}$ with the composition of the fluid buffered by the reaction. Pigage was also able to model prograde reactions responsible for the production of kyanite, the first appearance of sillimanite, and the disappearance of staurolite. In a separate study, Pigage (1982) used the linear regression technique to model probable sillimanite-forming reactions in pelitic schist from the Sauswap complex, British Columbia. The regression analysis, which is supported by textural criteria, indicates that fibrolite formed initially by the breakdown of staurolite and/or garnet with rutile as a reactant phase. When rutile was exhausted as a reactant phase, however, garnet became a product phase and continued growth of fibrolite was accompanied by the growth of a second generation of garnets. This is an excellent example of where regression analysis has aided in the interpretation of the prograde development of metamorphic minerals; in this case, the sequence was first generation garnet, which was resorbed and then followed by growth of second generation garnets.

Fletcher and Greenwood (1979) applied regression analysis to progressively metamorphosed pelitic schists from the Penfold Creek Area,

British Columbia. Their approach was to use regression techniques to detect reaction relations within and between mineral assemblages. Only three assemblages analyzed by Fletcher and Greenwood contained evidence of linear dependence, and thus the capacity of buffering H_2O , whereas the remainder of the samples studied did not have the capability of buffering H_2O . Their results contrast with the findings of Pigage (1976) who found evidence that pelitic schists commonly have a capability to buffer $\mu(H_2O)$. In contrast with Pigage (1976), but in accord with Pigage (1982), Fletcher and Greenwood found rutile to be a reactant phase during growth of Al_2SiO_5 in the progressive metamorphism of pelitic schist.

Laird (1980) used regression techniques in a somewhat different way to model whole-rock reactions during the progressive metamorphism of mafic schist from Vermont. Measured mineral compositions in the "common" assemblage amphibole + chlorite + epidote + plagioclase + quartz + Ti phase + Fe^{3+} oxide + carbonate + K-mica from different metamorphic grades were used to calculate the weight percent of minerals in two "average" bulk compositions. The results of these calculations were plots of calculated weight percent of minerals against metamorphic grade, and they graphically depict the change in modal mineralogy with metamorphic grade. From these calculations, generalized continuous "whole-rock" reactions between different metamorphic zones were deduced. For example, between the garnet-albite and garnet-oligoclase zones the whole-rock reaction was



Whole-rock reactions were determined for low-, medium-, and high-pressure P-T paths. Thompson et al. (1982; also see Thompson, this volume) have factored these reactions into component parts.

In summary, least-squares modeling of metamorphic mineral assemblages has been used in two major ways. (1) The evaluation of linear dependencies *within* mineral assemblages has been used to confirm or disprove the validity of graphical projections, to determine the true variance of a mineral assemblage, and to evaluate the potential of an assemblage to buffer the chemical potential of volatile species. (2) Examination of linear dependencies *between* assemblages has led to determination of whether mineral assemblages overlap in composition space (the n-dimensional tie-line problem). This information is a necessary prerequisite to determining whether two mineral assemblages at different metamorphic grade can be related by an isochemical prograde mineral reaction, or whether essential differences in bulk composition exist

between the two assemblages. With this information as a starting point, linear regression analysis has been used to deduce overall prograde metamorphic reactions.

Linear regression analysis is an extremely powerful tool and is ideally suited for petrologic problems where measured mineral compositions are involved. However, there are pitfalls. For example, in order to deduce a whole-rock reaction, the compositions of the phases participating in the reaction must be specified. In the above-mentioned studies, rim compositions were always used, but these may not necessarily be the composition of the phases that participated in the reaction. Moreover, it is not always clear that a particular phase should even be included in a reaction. Consequently, careful textural analysis and mineral zoning studies are indispensable to ensure that the reaction which evolves from the regression analysis is consistent with observed sequences of mineral growth.

Pigage (1976,1982) has also emphasized the difficulty in evaluating the significance of a reaction derived from regression analysis, especially where minor components are concerned. Regression errors (residuals) for minor components such as Zn in staurolite or Mn or Ca in garnet are often within the analytical error of the measurements. Because of this, Pigage concluded that a particular assemblage was univariant, and was a potential buffer of $\mu(H_2O)$, at least within analytical error of measurement. In this application, regression becomes a problem of determining the true variance of a mineral assemblage. As Pigage pointed out, the implication of the regression analysis is that if more precise analyses were possible (i.e., the error ellipsoid were smaller), then the assemblage might be of higher variance. Thus we have the concept, which follows directly from the statistical analysis of the quality of the regression, that the thermodynamic variance of a mineral assemblage is dependent on the analytical precision of the measured mineral compositions.

CONCLUSIONS

Linear algebra is an extremely powerful tool that can be applied to problems of n-dimensional analysis of composition space. Linear algebra has none of the limitations of graphical analysis, but it is not always easy to see how to formulate a problem algebraically. The goal of this paper has been to provide some insight into how petrologic problems can be formulated. The one most significant conclusion is that almost all petrologic applications of linear algebra can be described as linear mapping of

a mineral composition vector from one set of coordinate axes into another. The mathematics necessary to solve diverse problems such as component transformations, balancing chemical reactions and petrologic mixing problems are, therefore, fundamentally identical. In the future, new applications of linear algebra to petrology beyond those discussed here should further enhance our insights into the complexities of the composition space of metamorphic mineral assemblages.

ACKNOWLEDGMENTS

The authors would like to acknowledge the helpful reviews of J. Selverstone, K. Kimball, J. Rice and H. Lang as well as the able typing of D. Frank and drafting of D. Hall. Partial support for this work was funded by National Science Foundation Grant EAR-8108617 (Spear) and a Joseph H. Defrees grant of the Research Corporation (Spear).

CHAPTER 3 REFERENCES

- Aitken, A.C. (1956) *Determinants and Matrices*. 9th ed., Oliver and Boyd, Ltd., Edinburgh.
- Albarede, F. and A. Provost (1977) Petrological and geochemical mass-balance equations: an algorithm for least-square fitting and general error analysis. *Computers and Geosciences* 3, 309-326.
- Albee, A.L. (1965a) Phase equilibria in three assemblages of kyanite-zone pelitic schists, Lincoln Mountain Quadrangle, Central Vermont. *J. Petrol.* 6, 246-301.
- _____ (1965b) A petrogenetic grid for the Fe-Mg silicates of pelitic schists. *Am. J. Sci.* 263, 512-536.
- Anton, H. (1973) *Elementary Linear Algebra*. John Wiley & Sons, Inc., New York.
- Banks, R. (1979) The use of linear programming in the analysis of petrological mixing problems. *Contrib. Mineral. Petrol.* 70, 237-244.
- Barker, F. (1961) Phase relations in cordierite-garnet-bearing Kinsman quartz monzonite and the enclosing schist, Lovewell Mountain Quadrangle, New Hampshire. *Am. Mineral.* 46, 1166-1176.
- Bence, A.E. and Albee, A.L. (1968) Empirical correction factors for the electron microanalysis of silicates and oxides. *J. Geol.* 76, 382-403.
- Bowen, N.L. (1940) Progressive metamorphism of siliceous limestone and dolomite. *J. Geol.* 48, 225-274.
- Brady, J.B. (1975) Reference frames and diffusion coefficients. *Am. J. Sci.* 275, 954-983.
- _____ and J.H. Stout (1980) Normalizations of thermodynamic properties and some implications for graphical and analytical problems in petrology. *Am. J. Sci.* 280, 173-189.
- Bryan, W.B., L.W. Finger, and F. Chayes (1969) Estimating proportions in petrographic mixing equations by least-squares approximation. *Science* 163, 926-927.
- Davis, J.C. (1973) *Statistics and Data Analysis in Geology*. John Wiley & Sons, Inc., New York.
- Draper, N. and H. Smith (1966) *Applied Regression Analysis*. John Wiley & Sons, Inc., New York.
- Engel, A.E.J. and G.G. Engel (1962a) Hornblendes formed during progressive metamorphism of amphibolites, Northwest Adirondack Mountains, New York. *Bull. Geol. Soc. Am.* 73, 1499-1514.
- _____, _____, and R.G. Havens (1964) Mineralogy of amphibolite interlayers in the Gneiss Complex, Northwest Adirondack Mountains, New York. *J. Geol.* 72, 131-156.
- Eskola, P. (1915) On the relations between the chemical and mineralogical composition in the metamorphic rocks of the Orjarvi region. *Bull. Comm. Geol. Finlande* 44.
- Ferry, J.M. (1979) A map of chemical potential differences within an outcrop. *Am. Mineral.* 64, 966-985.
- Fletcher, C.J.N. (1971) Local equilibrium in a two-pyroxene amphibolite. *Canadian J. Earth Sci.* 8, 1065-1080.
- _____ and H.J. Greenwood (1979) Metamorphism and structure of Penfold Creek area, near Quesnel Lake, British Columbia. *J. Petrol.* 20, 743-794.
- Gray, N.H. (1973) Estimation of parameters in petrologic materials balance equations. *J. Math. Geol.* 5, 225-236.
- Greenwood, H.J. (1967) The n-dimensional tie-line problem. *Geochim. Cosmochim. Acta* 31, 465-490.
- _____ (1968) Matrix methods and the phase rule in petrology. *XXII Internat. Geol. Cong.* 6, 267-279.
- _____ (1975) Thermodynamically valid projections of extensive phase relationships. *Am. Mineral.* 60, 1-8.
- Harte, B. (1975) Determination of a pelitic petrogenetic grid for the eastern Scottish Dalradian. *Carnegie Inst. Wash. Year Book* 74, 438-446.
- _____ and C.M. Graham (1975) The graphical analysis of greenschist to amphibolite facies mineral assemblages in metabasites. *J. Petrol.* 16, 347-370.
- Hess, P.C. (1969) The metamorphic paragenesis of cordierite in pelitic rocks. *Contrib. Mineral. Petrol.* 24, 191-207.
- Korzhinskii, D.S. (1959) *Physicochemical Basis of Analysis of the Paragenesis of Minerals*. Consultants Bureau, Inc., New York.
- Laird, J. (1980) Phase equilibria in mafic schist from Vermont. *J. Petrol.* 21, 1-37.

APPENDIX A

PROGRAM TETPLT: A FORTRAN Program to Plot Stereoscopic Phase Diagrams

Visualization of metamorphic mineral assemblages is greatly aided by graphical projections. Three-component phase diagrams are simple to draw, but accurate drawings of four-component tetrahedral phase diagrams are difficult without computer assistance. Spear (1980) presented an algorithm for converting four-component barycentric coordinates into spatial Cartesian coordinates (x-y-z) so that the tetrahedron may be plotted in stereoscopic perspective.

The FORTRAN program TETPLT contained in this appendix performs these calculations and generates stereoscopic drawings of tetrahedral phase diagrams from any perspective desired. The program will also plot triangular phase diagrams. The program is written to run under Dec's RT-11 operating system, but should be easily convertible to any operating system. It is an interactive program and will have to be modified to run under batch. The plotting subroutines are designed for a Hewlett-Packard HP 7221B 4-pen plotter, and are largely self-explanatory. The only information necessary to know about the plotting subroutines is that the scaling of the plot assumes an x-y plotting pattern of 15,000-10,000 (0.025 units/mm).

The only input necessary to run the program is a file containing the four component barycentric plotting coordinates of the minerals to be plotted. If a triangular plot is desired, then the fourth barycentric coordinate should be set equal to 0. The file must be structured like so:

```
TITLE OF PLOT (80 characters)
LABEL COMPONENT A
LABEL COMPONENT B
LABEL COMPONENT C
LABEL COMPONENT D
TITLE MINERAL 1
PLOTTING COORDINATES MINERAL 1
TITLE MINERAL 2
PLOTTING COORDINATES MINERAL 2
etc.
```

Running the program. Most commands are self-explanatory. However, the relationship between the input angles and the stereoscopic view that is drawn needs discussion. When the command to draw the tetrahedron is specified, the program asks

INPUT ALPHA, THETA, GAMMA, EYE DISTANCE and SCALE

The angles ALPHA and THETA control the rotation of the tetrahedron as shown in Figure A1 and can be any number $\pm 360^\circ$. GAMMA determines the amount of stereo shift and EYE DISTANCE determines the amount of foreshortening. Both these numbers should be about the same magnitude (e.g., 5 and 5 or 20 and 20) but can be adjusted to suit individual preference. SCALE is the parameter that determines the size of the tetrahedron. It corresponds to unit distance in plotter units, usually 4000 or 5000 on a plotter that has x-y limits of 15,000-10,000. If in doubt about what to type in, try ... 0, 0, 5, 5, 4000.

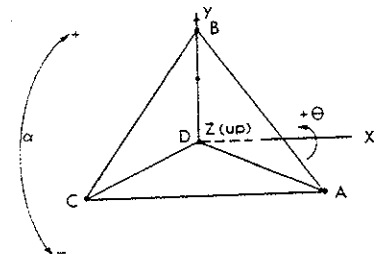


Figure A1. Relationship between the 4 barycentric coordinates A, B, C, and D and the 3 Cartesian coordinates X, Y, and Z used in the program TETPLT. Shown in the original orientation of the tetrahedron. The angle α is a \pm rotation around the Z axis and the angle θ is a \pm rotation around the X axis. Y, which determines the amount of stereo shift, is a \pm rotation around Y.

LeMaitre, R.W. (1979) A new generalized petrological mixing model. *Contrib. Mineral. Petrol.* 71, 133-137.

Palatnik, L.S. and A.I. Landau (1964) *Phase Equilibria in Multicomponent Systems*. Holt, Rinehart and Winston.

Perry, K.L., Jr. (1967a) An application of linear algebra to petrologic problems: Part 1. Mineral classification. *Geochim. Cosmochim. Acta* 31, 1043-1078.

____ (1967b) Methods of petrologic calculation and the relationship between mineral and bulk chemical composition. *Contrib. Geol.* 6, 5-38.

____ (1968a) Representation of mineral chemical analyses in 11-dimensional space. Part 1, Feldspars. *Lithos* 1, 201-218.

____ (1968b) Representation of mineral chemical analyses in 11-dimensional space. Part 2, Amphiboles. *Lithos* 1, 307-321.

Pigage, L.C. (1976) Metamorphism of the Settler Schist, southwest of Yale, British Columbia. *Canadian J. Earth Sci.* 3, 405-421.

____ (1982) Linear regression analysis of sillimanite-forming reactions. *Canadian Mineral.*, in press.

Reid, M.J., A.J. Gancarz, and A.L. Albee (1973) Constrained least-squares analysis of petrologic problems with an application to lunar sample 12040. *Earth Planet. Sci. Lett.* 17, 443-445.

Robinson, P. and H. Jaffe (1969) Chemographic exploration of amphibole assemblages from central Massachusetts and southwestern New Hampshire. *Spec. Pap. Mineral. Soc. Am.* 2, 251-274.

____, F.S. Spear, J.C. Schumacher, J. Laird, C. Klein, B.W. Evans, and B.L. Doolan (1982) Phase relations of metamorphic amphiboles: natural occurrence and theory. In D.R. Veblen, Ed., *Reviews in Mineralogy 9B*, Mineralogical Society of America, Washington, D.C.

Rumble, D., III (1977) Mineralogy, petrology and oxygen isotopic geochemistry of the Clough Formation, Black Mountain, Western New Hampshire, U.S.A. *J. Petrol.* 19, 317-340.

Skippen, G.B. (1974) An experimental model for low pressure metamorphism of siliceous dolomitic marble. *Am. J. Sci.* 274, 487-509.

Spear, F.S. (1982) Phase equilibria of amphibolites from the Post Pond Volcanics, Mt. Cube Quadrangle, Vermont. *J. Petrol.* 23, 383-426.

Stout, J. (1972) Phase petrology and mineral chemistry of coexisting amphiboles from Telemark, Norway. *J. Petrol.* 13, 99-145.

Strang, G. (1980) *Linear Algebra and Its Applications*, 2nd ed. Academic Press, New York.

Thompson, A. B. (1975) Mineral reactions in a calc-mica schist from Cassetts, Vermont, U.S.A. *Contrib. Mineral. Petrol.* 53, 105-127.

Thompson, J.B., Jr. (1957) The graphical analysis of mineral assemblages in pelitic schists. *Am. Mineral.* 42, 842-858.

____ and A.B. Thompson (1976) A model system for mineral facies in pelitic schists. *Contrib. Mineral. Petrol.* 58, 243-277.

Wright, T.L. and P.C. Doherty (1970) A linear programming and least squares computer method for solving petrologic mixing problems. *Bull. Geol. Soc. Am.* 81, 1995-2008.


```
PROGRAM TEST1
COMPILED BY F. SWEAR
UPDATE 2-FEB-82 TO INCLUDE TRIANGLE PLOTS
UPDATE MAY-82 FOR MSA SHORTCOURSE

-----DESCRIPTION OF PLOTTER ROUTINES-----
THE PLOTTER PLANNER IS DIVIDED INTO A 1500X1000X0 GRID IN THE
X AND Y DIRECTIONS. EACH PLOTTER UNIT = 0.025 MM.
THE PLOTTER SUBROUTINES ARE AS FOLLOWS:
C CALL PLOTS
C CALL PLOTT
C CALL POFF
C CALL POK
C CALL MOVE(X,Y,N)
C CALL SYMB(N,R,H)
C CALL LABSZ(N,H)
C CALL NENPEN(N)
C CALL PENUP
C STATEMENTS SUCH AS
C 100 PLOT(100,100) 126,39,.....,3
C WRITE A LABEL ONTO THE PLOT. ASCII CODE 126,39 TURNS THE LABEL
C INTO A LABEL AND 3 TURNS LABEL MODE OFF. EVERYTHING INBETWEEN IS A LABEL.
C THESE SUBROUTINES ARE NOT HP PLOT/21 SUBROUTINES BUT HERE CODED TO
C RUN AN HP-7221B PLOTTER ON A SMALL COMPUTER. THESE DESCRIPTIONS
C ARE GIVEN TO FACILITATE ADAPTATION OF THE PROGRAM TO ANOTHER PLOTTING
C SYSTEM. IF DESIRED, A COPY OF THE PLOTTING SUBROUTINES CAN BE
C OBTAINED BY WRITING THE AUTHOR.
C
C DIMENSION FLNAME(4)
C DIMENSION MINNO(12),PTITLE(40),APX(4,8),CI(4,4),LAB(8)
C DIMENSION BARY(4),TITLE(6,300)
C DIMENSION C(4,300),XLA(10),XRA(10),YLA(10),YRA(10)
C DIMENSION IINPUT
C NPRINT=5
C CALL PLOTS INITIALIZES THE PLOTTER
C CALL PLOTT
C CALL POFF
C SET DEFAULT STEREO VALUES
C ISHIFT=50
C ALPHA=0.
C THETA=0.
C ALL ANGLES ARE IN RADJANS. 57.29578 CONVERTS DEGS. TO RADJ.

0002 GAMMA=S./57.29578
0003 EYE=5.
0004 SCALE=5000.
0005 SET BARYCENTRIC COORDINATES FOR APICIES OF TETRAHEDRON
0006 DO 20 LJ=1,4
0007 DO 20 I=1,4
0008 C(I,I,LJ)=0.
0009 CI(LJ,LJ)=1.
0010 CONTINUE
0011 LJ=COUNTS THE # OF DATA POINTS IN THE DATA FILE
0012 TYPE *, 'INPUT FILE NAME FOR DATA'
0013 ACCEPT 62,FLNAME
0014 FORMAT(4A4)
0015 NFILE=1
0016 CALL ASSIGN (NFILE,FLNAME)
0017 READ TITLE OF PLOT
0018 READ TITLE(1,1),I=1,40
0019 FORMAT(40A1)
0020 DO 6 I=1,4
0021 READ(NFILE,1012)(APX(I,J),J=1,8),I=1,8)
0022 FORMAT(4A4)
0023 TYPE 2013,(APX(I,J),J=1,8),I=1,4)
0024 FC03(NFILE,1002)(END=99)(TITLE(I,LJ),I=1,8)
0025 FORMAT(2004)
0026 READ(NFILE,8)(C(I,LJ),I=1,4)
0027 PENORMALIZE BARYCENTRIC COORDINATES TO 1.0
0028 SUM=0
0029 DO 10 I=1,4
0030 SUM=SUM+C(I,LJ)
0031 IF(SUM.EQ.0)GO TO 18
0032 DO 15 I=1,4
0033 C(I,LJ)=C(I,LJ)/SUM
0034 CONTINUE
0035 TYPE 2015,(C(I,LJ),I=1,4),LJ,(TITLE(I,LJ),I=1,8)
0036 FORMAT(4F9.3,15',SXZ0R4)
0037 CONTINUE
0038 DO 10 I=1,4
0039 SUM=SUM+C(I,LJ)
0040 IF(SUM.EQ.0)GO TO 18
0041 DO 15 I=1,4
0042 C(I,LJ)=C(I,LJ)/SUM
0043 CONTINUE
0044 TYPE 2015,(C(I,LJ),I=1,4),LJ,(TITLE(I,LJ),I=1,8)
0045 FORMAT(4F9.3,15',SXZ0R4)
0046 CONTINUE
0047 DO 10 I=1,4
0048 SUM=SUM+C(I,LJ)
0049 IF(SUM.EQ.0)GO TO 18
0050 DO 15 I=1,4
0051 C(I,LJ)=C(I,LJ)/SUM
0052 CONTINUE
0053 GENERATE HARD COPY OF DATA FILE IF DESIRED
0054 NPR=0
0055 TYPE *, 'PRINT DATA???' I=YES, O=NO.
0056 ACCEPT *,NPR
0057 IF (NPR.EQ.0) GO TO 97
0058 PRINT 2012,(PTITLE(I),I=1,40)
0059 PRINT 2013,(APX(I,J),J=1,8),I=1,4)
0060 DO 96 I=1,LJ
0061 PRINT 2009,(C(I,J),J=1,4),I,(TITLE(I,J),J=1,8)
0062 FORMAT (' ',4F8.3,18,SX,8A4)
0063 CONTINUE
```

```
0108 Y=YLA(I)*SCALE+5000
0109 CALL MOVE(X,Y,1)
0110 WRITE(INPUT,333)126.39,(APX(I,J),J=1,8),3
0111 FORMAT ('',60A1,*)
0112 DO 3412
0113 DO 3412 I=1,4
0114 DO 3412 J=1,4
0115 X=YRA(I)*SCALE+11250+ISHIFT
0116 Y=YRA(I)*SCALE+5000
0117 CALL MOVE(X,Y,1)
0118 WRITE(INPUT,333)126.39,(APX(I,J),J=1,8),3
0119 CONTINUE
0120 CALL MOVE(Z0000.,9000.,1)
0121 WRITE(INPUT,333)126.39,(PTITLE(J),J=1,40),3
0122 RD=57.29578
0123 WRITE(INPUT,334)126.39,32.32,32.32,32.32,32.32,32.32,32.32,32.32.
0124 I,ALPHA,THETA,THETA,RD,GAMMA, EYE,SCALE,3
0125 FORMAT ('',11A1,SFB.1,A1)
0126 CALL POFF
0127 GO TO 3100
C ROUTINE TO PLOT ASSEMBLAGES CONNECTED BY TIE-LINES
C
0127 CONTINUE
0128 TYPE *, 'INPUT MINERAL NUMBERS TO PLOT.'
0129 TYPE *, 'FOLLOW EACH WITH A RETURN. END WITH 0.'
0130 NH=1
0131 ACCEPT *,MINNO(NH)
0132 IF (MINNO(NH).EQ.0)GO TO 200
0133 NH=NH+1
0134 GO TO 11
0135 CONTINUE
0136 NH=NH-1
0137 IF (NH.EQ.0)GO TO 3100
0138 DO 24 I=1,NH
0139 J=MINNO(I)
0140 DO 25 K=1,4
0141 BARY(K)=SCAL(J,K)
0142 DO 25 K=1,4
0143 XLA(I)=XL(J,K)
0144 YLA(I)=YL(J,K)
0145 XRA(I)=XR(J,K)
0146 YRA(I)=YR(J,K)
0147 CONTINUE
0148 TYPE *, 'INPUT PEN #'
0149 ACCEPT *,NOPEN
0150 GO TO 3000
C ROUTINE TO PLOT INDIVIDUAL POINTS WITH A LABEL
C
0153 CONTINUE
0154 DO 3610 I=1,9
0155 LABEL(I)=57 INPUT MINERAL # TO PLOT, 0 TO EXIT.
0156 ACCEPT *,K
0157
```

```
0108 CONTINUE
0109 CLOSE(UNIT=NFILE)
0110 TYPE *, 'TYPE 0 TO EXIT, 1 FOR TETRAHEDRAL PLOT, '
0111 TYPE *, ' 2 FOR TRIANGULAR PLOT, 3 TO INPUT NEW DATA FILE '
0112 ACCEPT *,ISK
0113 IF (ISK.EQ.0)GO TO 999
0114 GO TO (3100,5000,22)154
0115 GO TO 1
C THIS SECTION IS FOR TETRAHEDRAL PLOTS
C
0123 CONTINUE
0124 TYPE *, 'TETRAHEDRON PLOTTING ROUTINE.'
0125 TYPE *, 'YOUR OPTIONS ARE: 0=EXIT, 1=INPUT ANGLES,'
0126 * ' 2=PLOT ASSEMBLAGES, 4=PLOT POINTS,'
0127 TYPE *, 'INPUT OPTION...'
0128 ACCEPT *,IOPT
0129 IF (IOPT.EQ.0) GO TO 1
0130 GO TO (3300,3400,3500,3600)IOPT
0131 GO TO 3100
C ROUTINE TO INPUT ANGLES
C
0133 CONTINUE
0134 TYPE *, 'INPUT ALPHA,THETA,GAMMA,EYE DISTANCE AND SCALE '
0135 TYPE *, '(IF IN DOUBT, TYPE 0.0,0.0,57.3,0.000)'
0136 ACCEPT *,ALPHA,THETA,GAMMA,EYE,SCALE
0137 ALPHA=ALPHA/57.29578
0138 THETA=THETA/57.29578
0139 GAMMA=GAMMA/57.29578
0140 GO TO 3100
C ROUTINE TO PLOT TETRAHEDRON
C
0139 CONTINUE
0140 DO 60 I=1,4
0141 DO 52 K=1,4
0142 BARY(K)=C(I,K)
0143 CALL PROJEC(BARY,ALPHA,THETA,GAMMA,EYE,XL,YL,XR,YR)
0144 XLA(I)=XL
0145 YLA(I)=YL
0146 XRA(I)=XR
0147 YRA(I)=YR
0148 CONTINUE
0149 NH=4
0150 GO TO 3000
0151 CONTINUE
0152 DO 3410
0153 CALL LABSIZ(100.,200.)
0154 DO 3412 I=1,4
0155 X=YLA(I)*SCALE+3750+ISHIFT
```


This program solves a system of linear equations by matrix inversion techniques. The program has two options: invert matrix or solve a system of linear equations of the form $A \cdot X = Y$. The program can be used in component transformation problems or to balance chemical reactions.

Input is straightforward and self-explanatory. The program requests the dimensions of the matrix and then asks for the coefficient matrix A to be input by columns (i.e., mineral by mineral). Input is free format. If a system of equations is to be solved, the program also requests the data vector Y. The program then prints out the input matrix A, the inverse of this matrix A^{-1} , the determinant of A, and the data vector Y and solution vector X if necessary.

```

0001 C PROGRAM CALCULATES EITHER THE INVERSE OF A SQUARE MATRIX
0002 C OR SOLVES A SYSTEM OF LINEAR EQUATIONS BY POST MULTIPLICATION
0003 C OF THE INVERSE OF THE COEFFICIENTS MATRIX BY THE DATA VECTOR Y
0004
0005 REAL*8 A,DETA,Y,SUM,X
0006 DIMENSION A(20,20),IR(20),IC(20),Y(20),X(20)
0007 DIMENSION TITLE(20)
0008 1 CONTINUE
0009 TYPE *, 'INPUT TITLE'
0010 READ (5,1026,END=999) TITLE
0011 FORMAT (20A1)
0012 WRITE (6,1234) TITLE
0013 1234 FORMAT ('',////,20A4)
0014 TYPE *, 'INPUT MATRIX DIMENSION (N FOR NXN):TYPE 0 TO EXIT'
0015 READ(5,*,END=999) MA
0016 IF(MA.EQ.0)GO TO 999
0017 TYPE *, 'INPUT MATRIX BY COLUMNS. A RETURN AFTER EACH COLUMN'
0018 DO 10 I=1,MA
0019 10 READ(5,*) (A(I,J),J=1,MA)
0020 TYPE *, 'TYPE 0 FOR INVERSE ONLY, 1 FOR SOLUTION TO EQUATIONS'
0021 ACCEPT *,ITYPE
0022 IF (ITYPE.EQ.0) GO TO 100
0023 TYPE *, 'INPUT DATA VECTOR, Y'
0024 ACCEPT *,(Y(I),I=1,MA)
0025 CONTINUE
0026 WRITE (6,2005)
0027 2005 FORMAT('', ' INPUT COEFFICIENTS MATRIX '///)
0028 DO 15 I=1,MA
0029 15 WRITE(6,2010) (A(I,J),J=1,MA)
0030 2010 FORMAT ('', '14F9.5)
0031 DETA=0.0
0032 IER=0.0
0033 CALL MINURS(A,MA,DETA,IER,IR,IC)
0034 IF (IER.EQ.1) GO TO 50
0035 WRITE(6,2043)
0036 2043 FORMAT('', ' INVERSE OF COEFFICIENTS MATRIX'///)
0037 DO 20 I=1,MA
0038 20 WRITE(6,2010) (A(I,J),J=1,MA)
0039 WRITE (6,2020) ,DETA
0040 2020 FORMAT ('', ' DETERMINANT= ',F10.4)
0041 IF (ITYPE.EQ.0) GO TO 1
0042 WRITE (6,2314) (Y(I),I=1,MA)
0043 2314 FORMAT ('', ' ..... DATA VECTOR, Y .....',14F9.5)
0044 DO 150 I=1,MA
0045 150 SUM=0.0
0046 DO 155 J=1,MA
0047 155 SUM=SUM+A(I,J)*Y(J)
0048 X(I)=SUM
0049 150 X(I)=SUM
0050 WRITE (6,2313) (X(I),I=1,MA)
0051 2313 FORMAT ('', ' ..... SOLUTION VECTOR .....',14F9.5)
0052 GO TO 1
0053 50 WRITE(6,2000)
0054 2000 FORMAT ('', ' ..... MATRIX IS SINGULAR ..... ABORT')
0055 GO TO 1
0056 999 CONTINUE
0057 999

```

```

0001 SUBROUTINE MINURS (A,IA,JA,DETA,IER,IR,IC)
0002 REAL*8 A,PIV,DETA,PIV1,TEMP
0003 DIMENSION A(IA,IA),IR(MA),IC(MA)
0004 IER=0
0005 DO 1 I=1,MA
0006 IR(I)=0
0007 1 IC(I)=0
0008 DETA=1.0
0009 DO 123 IJKL=1,MA
0010 CALL SUBMKS (A,IA,IA,MA,MA,IR,IC,I,J)
0011 PIV=A(I,J)
0012 DETA=PIV*DETA
0013 IF (PIV.EQ.0.0) GO TO 17
0014 IR(I)=J
0015 IC(J)=I
0016 PIV=1.0/PIV
0017 DO 5 K=1,MA
0018 5 A(I,K)=A(I,K)*PIV
0019 A(I,J)=PIV
0020 DO 9 K=1,MA
0021 9 IF (K.EQ.I) GO TO 9
0022 PIV=A(K,J)
0023 6 DO B L=1,MA
0024 8 A(K,L)=A(K,L)-PIV*A(I,L)
0025 A(K,J)=PIV
0026 CONTINUE
0027 PIV=A(I,J)
0028 DO 11 K=1,MA
0029 11 A(K,J)=PIV*A(K,J)
0030 A(I,J)=PIV
0031 123 CONTINUE
0032 12 DO IS I=1,MA
0033 K=IC(I)
0034 M=IR(I)
0035 IF (K.EQ.I) GO TO 16
0036 DETA=DETA
0037 DO 14 L=1,MA
0038 14 A(K,L)=A(K,L)
0039 DO 15 L=1,MA
0040 15 A(L,M)=A(L,M)
0041 IC(K)=K
0042 IR(K)=M
0043 16 CONTINUE
0044 RETURN
0045 17 IER=1
0046 RETURN
0047 END
0048
0049 SUBROUTINE SUBMKS (A,IA,JA,MA,NA,IR,IC,I,J)
0050 REAL*8 A,X,TEST
0051 DIMENSION A(IA,JA),IR(MA),IC(MA)
0052 I=0
0053 J=0
0054 TEST=0.0
0055 DO 5 K=1,MA
0056 5 IF (IR(K).NE.0) GO TO 5
0057 DO 4 L=1,NA
0058 4 IF (IC(L).NE.0) GO TO 4
0059 X=DABS(A(K,L))
0060 IF (X.LT.TEST) GO TO 4
0061 L=K
0062 J=L
0063 TEST=X
0064 CONTINUE
0065 CONTINUE
0066 RETURN
0067 END

```

(PROGRAM LINEQU
CODED BY F. SPEAR
UPDATE APRIL 20, 1982)

ANALYTICAL FORMULATION OF PHASE EQUILIBRIA: THE GIBBS' METHOD

F.S. Spear, J.M. Ferry, and D. Rumble III

Chapter 4 INTRODUCTION

A basic goal in the study of metamorphic rocks is to characterize intensive variables during metamorphic events. The fundamental assumption that allows extraction of estimates of intensive variables from mineral assemblages is that the mineral phases attained a state of chemical equilibrium at some condition of elevated temperature and pressure during metamorphism. Furthermore, it is assumed that the compositions of minerals in rocks have not significantly changed from the time that they attained this high temperature-pressure equilibrium state. There are obviously numerous objections to these two assumptions: (a) Metamorphism is a dynamic process and there is little to assure that all or even most mineral compositions freeze in at the same point on the pressure-temperature-time path of a particular metamorphic rock; (b) rocks may have a polymetamorphic history with some mineral compositions the product of one event and other compositions the product of a second event; (c) reaction rates, diffusion rates, and/or rates of heat transfer may be too slow for minerals in a rock to ever attain chemical equilibrium at any time during a metamorphic event; etc. While many metamorphic rocks undoubtedly suffer from these problems, it is remarkable the number of studies that have found metamorphic rocks to be consistent with attainment of chemical equilibrium at some condition of elevated temperature and pressure.

Classical chemical thermodynamics constitutes a comprehensive mathematical framework in which intensive variables—temperature, pressure, chemical potential, phase composition—are related in a system at chemical equilibrium. Much of our modern understanding of metamorphism derives from a two-step exercise: (1) assumption that minerals in metamorphic rocks constitute a chemical system in a fossilized state of equilibrium; and (2) application of chemical thermodynamics to that rock system. The compositions of minerals in metamorphic rocks constitute certain intensive variables of the high temperature-pressure metamorphic state of equilibrium. Thermodynamic links these composition variables to other intensive variables of interest, which no longer may be directly determined (e.g., temperature and pressure). Through these links, it is thus possible to use mineral assemblages and compositions of minerals to reconstruct the value of those intensive